TABLE E2. List of SNPs carried out in a statistical search for interactions

Symbol	Name	Chr	RefSeq allele	Note
PTGER3	Prostaglandin E receptor EP3	chr1		
.	rs17131450		A/G	Genomic
	rs5702		C/T	Synonymous
	rs1325949		A/G	Intronic
	rs7543182		A/C	Intronic
	rs7555874		C/T	Intronic
	rs4147114		C/G	Intronic
	rs1327464		A/G	
IL13	Interleukin 13	chr5		
	rs1800925		C/T	Genomic
	rs20541		C/T	Missense
	rs1295685		C/T	3'UTR
TLR3	Toll-like receptor 3	chr4		
	rs3775296		G/T	Intronic
	rs3775295		C/T	Intronic
	rs3775294		C/T	Intronic
	rs3775293		C/T	Intronic
	rs3775292		C/G	Intronic
	rs3775291		A/G	Missense
	rs3775290		A/G	Intronic
FasL	Fas ligand	chr1		
	rs3830150		A/G	Intron of C1orf9
	rs2859247		C/T	Genomic
	rs2639614		A/G	Genomic
	rs929087		A/G	Intronic
IL4R	Interleukin 4 receptor	chr16		
	rs1805010		A/C/G/T	Missense
	rs1805015		C/T	Missense
	rs1801275		A/G	Missense
MAIL	Nuclear factor of kappa light polypeptide gene enhancer in B-cells inhibitor, zeta	chr3		
	rs3821727		C/G	Missense
	rs677011		A/G	Intronic
	rs595788		C/T	Intronic
	rs3217713		indel	Intronic
	rs14134		A/G	Synonymous
	rs622122		A/T	Intronic
	rs2305991		A/G	3'UTR
IL4	Interleukin 4	chr5		
	rs2243250		C/T	
IL1A	Interleukin 1, alpha	chr2		
	rs2071376		A/C	Intronic
	rs2071375		A/G	Intronic
	rs2071373		C/T	Intronic
	rs1894399		A/G	Intronic
	rs1609682		A/C	Intronic
TLR2	Toll-like receptor 2	chr4		
	rs3804100			Synonymous
	rs3804099			Synonymous
TLR5	Toll-like receptor 5	chr1		
	rs2072493		A/G	Missense
	rs5744168		A/C/G/T	STOP
PTGER4	Prostaglandin E receptor 4	chr5		
	rs1494558		A/C/G/T	Missense
Chr5p13	Genes in cytogenetic band chr5p13	chr5		
	rs6871834		A/G	Genomic
GNLY	Granulysin	chr2		
	rs3755007		A/C	Genomic

TABLE E3. Susceptible interactions between loci detected by using Interactive Sure Independence Screening

Locus 1	Locus 2	OR	95% CI	P value
PTGER3 **rs4147114 (GC)**	*TLR3* **rs3775296 (TT)**	**25.3**	**3.2-203**	**.0000527**
PTGER3 rs4147114 (GC)	—	2.66	1.4-5.0	.0023
—	*TLR3* rs3775296 (TT)	5.35	2.0-14.1	.00025
*HLA-A*02:06*	*IL1A* **rs1609682 (CA)**	**9.66**	**2.0-47.0**	**.00193**
*HLA-A*02:06*	—	3.46	1.8-6.8	.0002
—	*IL1A* rs1609682 (CA)	—	—	.31

Boldface text indicates the pairs with interactions.

TABLE E4. Association between *TLR3* SNPs and SJS/TEN with ocular complications

rs no. of SNP	Genotypes		Frequencies of genotypes (%) Controls	Cases	Allele 1 vs allele 2 *P* value* OR (95% CI)	Genotype 11 vs 12+22 *P* value* OR (95% CI)	Genotype 11+12 vs 22 *P* value* OR (95% CI)
rs4861699	11	G/G	39.8	58.6	.0018	.001	.17
	12	G/A	47.5	33.6	1.76 (1.2-2.5)	2.14 (1.4-3.4)	—
	22	A/A	12.7	7.8			—
rs6822014	11	A/A	61.9	50.5	.00071	.048	.00008
	12	A/G	33.9	32.4	0.54 (0.4-0.8)	0.63 (0.4-1.0)	0.21 (0.1-0.5)
	22	G/G	4.2	17.1			
rs11732384	11	G/G	51.6	65.5	.032	.014	.68
	12	G/A	41.2	28.4	1.52 (1.0-2.2)	1.78 (1.1-2.8)	—
	22	A/A	7.2	6.0			—
rs3775296†	11	G/G	51.6	44.0	.0046	.18	.00009
	12	G/T	43.0	37.1	0.61 (0.4-0.9)	—	0.25 (0.1-0.5)
	22	T/T	5.4	19.0		—	
rs5743312	11	C/C	54.1	46.6	.0059	.19	.0001
	12	C/T	41.4	36.2	0.62 (0.4-0.9)	—	0.23 (0.1-0.5)
	22	T/T	4.6	17.2		—	
rs7668666	11	C/C	39.4	30.4	.01	.11	.0069
	12	C/A	47.9	45.2	0.65 (0.5-0.9)	—	0.45 (0.3-0.8)
	22	A/A	12.7	24.3		—	
rs3775290†	11	G/G	38.5	34.5	.057	.47	.0069
	12	G/A	50.2	43.1	—	—	0.44 (0.2-0.8)
	22	A/A	11.3	22.4	—	—	

P value for allele or genotype frequency comparison between cases and controls by using the χ^2 test.
†Italic rs numbers show previously reported SJS/TEN-associated SNPs.

TABLE E5. Association between *PTGER3* SNPs and SJS/TEN with ocular complications

rs no. of SNP	Genotypes		Frequencies of genotypes (%)		Allele 1 vs allele 2 P value* OR (95% CI)	Genotype 11 vs 12+22 P value* OR (95% CI)	Genotype 11+12 vs 22 P value* OR (95% CI)
			Controls	Cases			
rs7555865	11	C/C	47.9	45.7	.10	.69	.0083
	12	C/T	42.5	34.5	—	—	0.43 (0.2-0.8)
	22	T/T	9.6	19.8	—	—	
rs17131450†	11	C/C	87.8	76.7	.00069	.0086	.0039
	12	C/T	11.8	18.1	0.41 (0.2-0.7)	0.46 (0.3-0.8)	0.08 (0.01-0.7)
	22	T/T	0.5	5.2			
rs5702†	11	C/C	49.3	64.7	.059	.0072	.6
	12	C/T	43.0	25.9	—	1.88 (1.2-3.0)	—
	22	T/T	7.7	9.5	—	—	—
rs1325949†	11	A/A	47.5	69.0	.0035	.00017	.88
	12	A/G	44.3	22.4	1.8 (1.2-2.6)	2.5 (1.5-3.9)	—
	22	G/G	8.1	8.6			—
rs2421805	11	T/T	48.1	33.6	.0014	.012	.0045
	12	T/G	44.4	48.7	0.58 (0.4-0.8)	0.55 (0.3-0.9)	0.37 (0.2-0.8)
	22	G/G	7.4	17.7			
rs7543182†	11	G/G	50.7	70.7	.0096	.00041	.54
	12	G/T	42.5	20.7	1.67 (1.1-2.5)	2.34 (1.5-3.8)	—
	22	T/T	6.8	8.6			—
rs.7555874†	11	G/G	50.7	69.8	.014	.00074	.54
	12	G/A	42.5	21.6	1.62 (1.1-2.4)	2.25 (1.4-3.6)	—
	22	A/A	6.8	8.6			—
rs1409981	11	G/G	84.7	73.3	.0021	.012	.040
	12	G/A	13.0	19.8	0.48 (0.3-0.8)	0.49 (0.3-0.9)	0.32 (0.1-1.0)
	22	A/A	2.3	6.9			
rs.4147114†	11	C/C	24.4	43.1	.0012	.00042	.10
	12	C/G	53.4	42.2	1.72 (1.2-2.4)	2.34 (1.5-3.8)	—
	22	G/G	22.2	14.7			—
rs4147115	11	A/A	25.5	39.5	.023	.0098	.34
	12	A/T	46.7	37.6	1.46 (1.1-2.0)	1.91 (1.2-3.1)	—
	22	T/T	27.8	22.9			—
rs4650093	11	C/C	51.4	65.5	.092	.013	.44
	12	C/T	42.3	25.9	—	1.8 (1.1-2.9)	—
	22	T/T	6.4	8.6	—		—
rs17131478	11	G/G	61.6	74.6	.035	.018	.79
	12	G/T	34.2	21.9	1.59 (1.0-2.5)	1.8 (1.1-3.0)	—
	22	T/T	4.1	3.5			—
rs17131479	11	C/C	62.2	75.0	.039	.018	.91
	12	C/G	34.1	21.6	1.58 (1.0-2.4)	1.8 (1.1-3.0)	—
	22	G/G	3.7	3.4			—
rs7521005	11	A/A	51.6	65.5	.10	.014	.44
	12	A/G	42.1	25.9	—	1.8 (1.1-2.8)	—
	22	G/G	6.3	8.6	—		—
rs7541092	11	G/G	62.4	74.8	.040	.023	.77
	12	G/A	33.5	21.7	1.57 (1.0-2.4)	1.8 (1.1-3.0)	—
	22	A/A	4.1	3.5			—
rs1359835	11	G/G	88.6	79.1	.0047	.019	.030
	12	G/C	10.9	17.4	0.45 (0.3-0.8)	0.49 (0.3-0.9)	0.13 (0.01-1.1)
	22	C/C	0.5	3.5			
rs1327464	11	G/G	88.2	78.4	.0043	.017	.031
	12	G/A	11.3	18.1	0.46 (0.3-0.8)	0.49 (0.3-0.9)	0.13 (0.01-1.1)
	22	A/A	0.5	3.4			
rs1409161	11	G/G	30.8	25.9	.040	.35	.014
	12	G/A	51.6	44.8	0.72 (0.5-1.0)	—	0.52 (0.3-0.9)
	22	A/A	17.6	29.3		—	
rs34885906	11	T/T	85.5	94.0	.026	.021	.0
	12	T/C	14.5	6.0	2.5 (1.1-5.8)	2.6 (1.1-6.2)	—
	22	C/C	0.0	0.0	—		—
rs2817864	11	T/T	53.4	61.2	.056	.17	.021
	12	T/G	40.3	37.9	—	—	7.8 (1.0-59.9)
	22	G/G	6.3	0.9	—	—	

*P value for allele or genotype frequency comparison between cases and controls by using the χ^2 test.
†Italic rs numbers show previously reported SJS/TEN-associated SNPs.

RESEARCH LETTERS

Downregulation of Monocyte Chemoattractant Protein 1 Expression by Prostaglandin E₂ in Human Ocular Surface Epithelium

Elsewhere, we reported that in the tears and serum of patients with acute-stage Stevens-Johnson syndrome or toxic epidermal necrolysis, the levels of interleukin 6 (IL-6), IL-8, and monocyte chemoattractant protein 1 (MCP-1) were dramatically increased.[1] We also reported that Stevens-Johnson syndrome or toxic epidermal necrolysis with severe ocular complications was associated with polymorphism of the prostaglandin E receptor 3 (EP₃) gene (PTGER3).[2]

Prostanoids are a group of lipid mediators that form in response to various stimuli. They include prostaglandin D₂ (PGD₂), PGE₂, PGF₂ₐ, PGI₂, and thromboxane A₂. There are 4 subtypes of the PGE receptor: EP₁, EP₂, EP₃, and EP₄. We previously reported that PGE₂ suppresses polyinosine–polycytidylic acid (polyI:C)–stimulated cytokine production via EP₂ and/or EP₃ in human ocular surface epithelial cells.[3,4] PolyI:C is a ligand of Toll-like receptor 3, which is strongly expressed in ocular surface epithelium.[5] We found that PGE₂ suppresses the production of IL-6, chemokine (C-X-C motif) ligand 10, chemokine (C-X-C motif) ligand 11, and chemokine (C-C motif) ligand 5 but not IL-8 by epithelial cells on the human ocular surface[3]; it remains to be determined whether it also suppresses MCP-1 production. Monocyte chemoattractant protein 1 plays a significant role in the recruitment of monocytes and lymphocytes to the site of cellular immune reactions. In this study, we investigated whether PGE₂ downregulates polyI:C-induced MCP-1 production.

All experiments were conducted in accordance with the principles set forth in the Declaration of Helsinki. Enzyme-linked immunosorbent assay and quantitative real-time polymerase chain reaction were performed with primary human conjunctival epithelial cells and immortalized human corneal-limbal epithelial cells using previously described methods (eAppendix, http://www.archophthalmol.com).[3]

First, we examined whether PGE₂ downregulated the production and messenger RNA (mRNA) expression of MCP-1 induced by polyI:C stimulation in human conjunctival and corneal epithelial cells. We found that it significantly attenuated the production of MCP-1 (**Figure**, A). Quantitative real-time polymerase chain reaction confirmed that the mRNA expression of MCP-1 was significantly downregulated by PGE₂ (Figure, A).

Next, we examined which PGE₂ receptor(s) contributed to the downregulation of polyI:C-induced MCP-1. We used the EP₂ agonist ONO-AE-259, the EP₃ agonist ONO-AE-248, and the EP₄ agonist ONO-AE-329. Enzyme-linked immunosorbent assay showed that the EP₂ and EP₃ agonists significantly suppressed the polyI:C-induced production of MCP-1, while the EP₄ agonist did not exert suppression (Figure, B). Quantitative real-time polymerase chain reaction confirmed that the EP₂ and EP₃ agonists significantly downregulated the mRNA expression of MCP-1 (Figure, C). Thus, our results document that PGE₂ attenuated the mRNA expression and production of MCP-1 via both EP₂ and EP₃.

In human macrophages, PGE₂ attenuated the lipopolysaccharide-induced mRNA and protein expression of chemokines including MCP-1 through EP₄.[6] On the other hand, we demonstrated that in human ocular surface epithelial cells, PGE₂ attenuated the polyI:C-induced mRNA and protein expression of MCP-1 through EP₂ and EP₃ but not EP₄. Our findings suggest that EP₂ and EP₃ play important roles in the regulation of inflammation in epithelial cells, while EP₂ and EP₄ have important roles in immune cells such as macrophages.

In the tears and serum of patients with acute-stage Stevens-Johnson syndrome or toxic epidermal necrolysis, the levels of IL-6, IL-8, and MCP-1 were dramatically increased.[1] Although IL-8 was not regulated by PGE₂, IL-6 was regulated by PGE₂ via EP₃ in human ocular surface epithelial cells.[3] Herein, we demonstrated that MCP-1 could be regulated by PGE₂ via EP₂ and EP₃. The regulation of cytokine production by PGE₂ may be associated with the pathogenesis of Stevens-Johnson syndrome or toxic epidermal necrolysis with severe ocular complications because it was associated with polymorphism of the EP₃ gene (PTGER3), one of the PGE receptors (EP₁, EP₂, EP₃, EP₄).[2]

In summary, our results show that MCP-1 produced by human ocular surface epithelial cells could be downregulated by PGE₂ via EP₂ and EP₃.

Mayumi Ueta, MD, PhD
Chie Sotozono, MD, PhD
Norihiko Yokoi, MD, PhD
Shigeru Kinoshita, MD, PhD

Author Affiliations: Research Center for Inflammation and Regenerative Medicine, Faculty of Life and Medical Sciences, Doshisha University (Dr Ueta) and Department of Ophthalmology, Kyoto Prefectural University of Medicine (Drs Ueta, Sotozono, Yokoi, and Kinoshita), Kyoto, Japan.
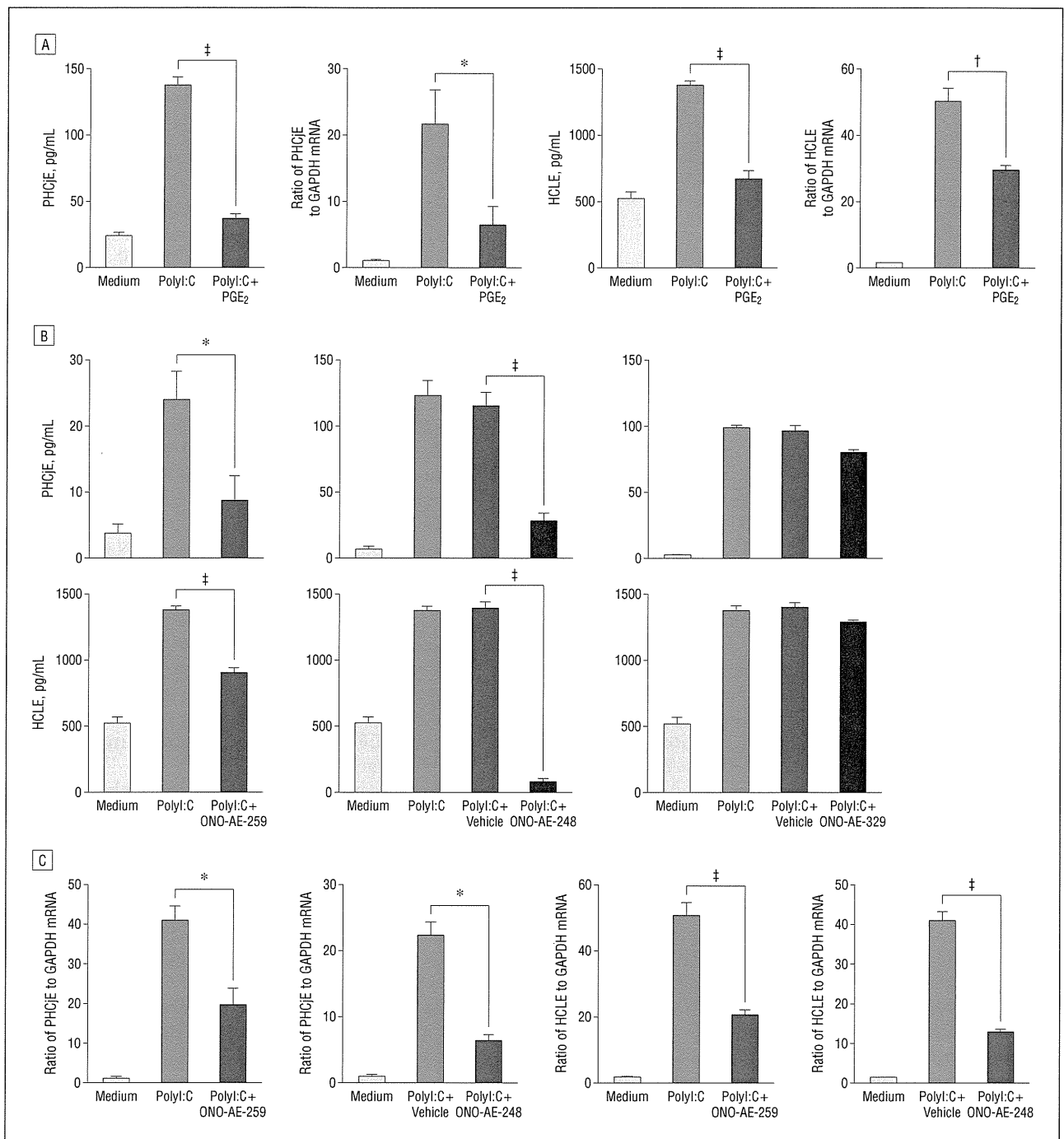**Correspondence:** Dr Ueta, Department of Ophthalmology, Kyoto Prefectural University of Medicine, 465 Ka-

Figure. Prostaglandin E_2 (PGE$_2$) attenuated the messenger RNA (mRNA) expression and production of monocyte chemoattractant protein 1 via both prostaglandin E receptor 2 (EP$_2$) and EP$_3$. A, Primary human conjunctival epithelial cells (PHCjE) and human corneal-limbal epithelial cells (HCLE) were exposed to 10 µg/mL of polyinosine–polycytidylic acid (polyI:C) and 100 µg/mL of PGE$_2$ for 24 hours (enzyme-linked immunosorbent assay) or 6 hours (quantitative real-time polymerase chain reaction). GAPDH indicates glyceraldehyde-3-phosphate dehydrogenase. B and C, The PHCjE and HCLE were exposed to 10 µg/mL of polyI:C and 10 µg/mL of the EP$_2$, EP$_3$, or EP$_4$ agonist for 24 hours (enzyme-linked immunosorbent assay) (B) or 6 hours (quantitative real-time polymerase chain reaction) (C). Data are representative of 3 separate experiments and are given as the mean (SEM) from 1 experiment carried out in 6 to 8 wells (enzyme-linked immunosorbent assay) (B) or 4 to 6 wells (quantitative real-time polymerase chain reaction) (C) per group. *$P<.05$; †$P<.005$; ‡$P<.001$.

jiicho, Hirokoji, Kawaramachi, Kamigyoku, Kyoto 602-0841, Japan (mueta@koto.kpu-m.ac.jp).
Author Contributions: Dr Ueta had full access to all of the data in the study and takes responsibility for the integrity of the data and the accuracy of the data analysis.

- 260 -

Shimizu Foundation for Immunological Research Grant.

1. Yagi T, Sotozono C, Tanaka M, et al. Cytokine storm arising on the ocular surface in a patient with Stevens-Johnson syndrome. Br J Ophthalmol. 2011; 95(7):1030-1031.
2. Ueta M, Sotozono C, Nakano M, et al. Association between prostaglandin E receptor 3 polymorphisms and Stevens-Johnson syndrome identified by means of a genome-wide association study. J Allergy Clin Immunol. 2010;126(6): 1218-1225, e10.
3. Ueta M, Matsuoka T, Yokoi N, Kinoshita S. Prostaglandin E2 suppresses polyinosine-polycytidylic acid (polyI:C)-stimulated cytokine production via prostaglandin E2 receptor (EP) 2 and 3 in human conjunctival epithelial cells. Br J Ophthalmol. 2011;95(6):859-863.
4. Ueta M, Matsuoka T, Yokoi N, Kinoshita S. Prostaglandin E receptor subtype EP3 downregulates TSLP expression in human conjunctival epithelium. Br J Ophthalmol. 2011;95(5):742-743.
5. Ueta M, Kinoshita S. Innate immunity of the ocular surface. Brain Res Bull. 2010;81(2-3):219-228.
6. Takayama K, García-Cardena G, Sukhova GK, Comander J, Gimbrone MA Jr, Libby P. Prostaglandin E2 suppresses chemokine production in human macrophages through the EP4 receptor. J Biol Chem. 2002;277(46):44147-44154.

Depth Profile Study of Abnormal Collagen Orientation in Keratoconus Corneas

In a previous study,[1] we used femtosecond laser technology to cut ex vivo human corneas into anterior, mid, and posterior sections, after which x-ray scatter patterns were obtained at fine intervals over each specimen. Data analysis revealed the predominant orientation of collagen at each sampling site, which was assembled to show the variation in collagen orientation between central and peripheral regions of the cornea and as a function of tissue depth. We hypothesized that the predominantly orthogonal arrangement of collagen (directed toward opposing sets of rectus muscles) in the mid and posterior stroma may help to distribute strain in the cornea by allowing it to withstand the pull of the extraocular muscles. It was also suggested that the more isotropic arrangement in the anterior stroma may play a role in tissue biomechanics by resisting intraocular pressure while at the same time maintaining corneal curvature. This article, in conjunction with our findings of abnormal collagen orientation in full-thickness keratoconus corneas,[2,3] received a great deal of interest from the scientific community and prompted the following question: how does collagen orientation change as a function of tissue depth when the anterior curvature of the cornea is abnormal, as in keratoconus? Herein, we report findings from our investigation aimed at answering this question.

Methods. The Baron chamber used in our previous study[1] was adapted to enable corneal buttons to be clamped in place and inflated (by pumping physiological saline into the posterior compartment) to restore their natural curvature. A button diameter of 8 mm or larger was deemed necessary to ensure tissue stability during this process.

The next step, obtaining fresh, full-thickness, keratoconus buttons of sufficient diameter, proved to be problematic owing to the increasing popularity of deep anterior lamellar keratoplasty. Recently, however, the

opportunity arose to examine an 8-mm full-thickness (300-340 μm minus epithelium) keratoconus corneal button with some central scarring and a mean power greater than 51.8 diopters (**Figure 1**). The tissue was obtained in accordance with the tenets of the Declaration of Helsinki and with full informed consent from a 31-year-old patient at the time of penetrating keratoplasty. Using techniques detailed previously,[1] the corneal button was clamped in the chamber and inflated. The central 6.3-mm region of the button was then flattened by the applanation cone and a single cut was made at a depth of 150 μm from the surface using an IntraLase 60-kHz femtosecond laser (Abbott Medical Optics Inc),[1] thus splitting the cornea into anterior and posterior sections of roughly equal thickness. Wide-angle x-ray scattering patterns were collected at 0.25-mm intervals over each cor-
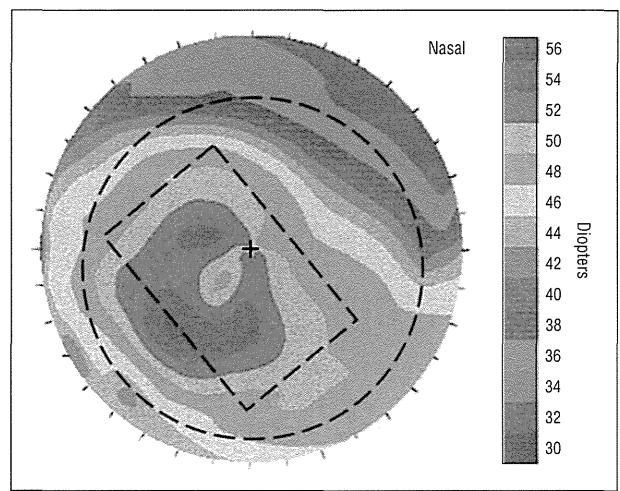

Figure 1. Corneal topography of the keratoconus cornea (recorded 12 years previously).[3] The broken lines show the 6.3-mm region of the cornea cut with the femtosecond laser (circle) and the region of greatest corneal steepening depicted in Figure 2 (rectangle).
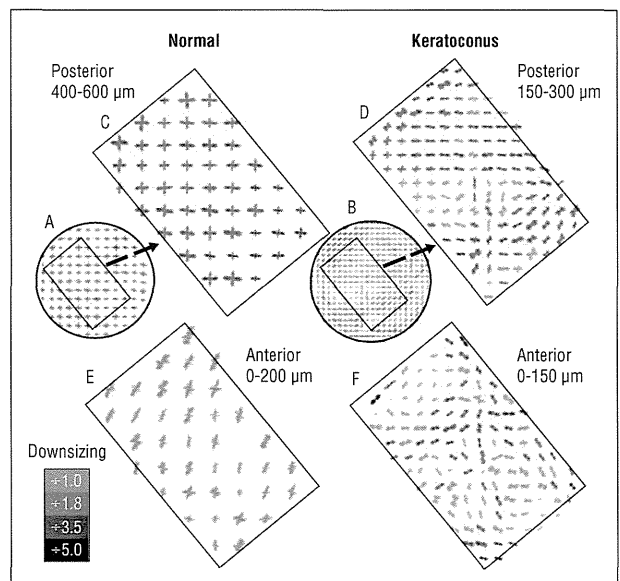

Figure 2. Collagen orientation in the normal (A) and keratoconus (B) posterior stroma (central 6.3 mm). The highlighted regions of the posterior (C and D) and anterior (E and F) stroma are expanded. Large vector plots showing high collagen alignment are downsized (key).

- 261 -

Epithelial and Mesenchymal Cell Biology

Functional Role of PPARδ in Corneal Epithelial Wound Healing

Yoshikuni Nakamura,* Takahiro Nakamura,†‡
Takeshi Tarui,* Jun Inoue,* and
Shigeru Kinoshita‡

From the Kobe Creative Center,* Senju Pharmaceutical Co., Ltd., Kobe; the Research Center for Inflammation and Regenerative Medicine,† Faculty of Life and Medical Sciences, Doshisha University, Kyoto; and the Department of Ophthalmology,‡ Kyoto Prefectural University of Medicine, Kyoto, Japan

The peroxisome proliferator-activated receptor (PPAR) δ is involved in tissue repair. In this study, we investigated the functional role of PPARδ in corneal epithelial wound healing. In an *in vivo* corneal wound-healing model, the changes of PPARδ expression in corneal epithelia were examined by immunofluorescence microscopy, and the effect of topical administrations of a PPARδ agonist on corneal wound healing was also evaluated. The inhibitory effect of a PPARδ agonist on the cytokine-induced death of human corneal epithelial cells was evaluated using a DNA fragmentation assay kit. The changes of PPARδ expression and epithelial cell death were also investigated using human corneoscleral tissues *ex vivo*. Our findings showed that PPARδ expression was temporally up-regulated in corneal epithelial cells during experimental wound healing and that topical administration of a PPARδ agonist significantly promoted the healing of experimental corneal epithelial wounds. In human corneal epithelial cells, up-regulation of PPARδ and DNA fragmentation was demonstrated by stimulation with cytokines, and the DNA fragmentation was significantly inhibited by pretreatment with a PPARδ agonist. By using human corneoscleral tissues *ex vivo*, PPARδ was up-regulated in both healthy corneal epithelia (during re-epithelialization) and diseased corneal epithelia. Inflammatory stimulation–induced corneal epithelial cell death was inhibited by pretreatment with a PPARδ agonist. These results strongly suggest that PPARδ is involved in the corneal epithelial wound healing. *(Am J Pathol 2012, 180:583–598; DOI: 10.1016/j.ajpath.2011.10.006)*

Peroxisome proliferator-activated receptors (PPARs) are ligand-activated transcription factors belonging to the nuclear hormone receptor family. The three isotypes of these transcription factors, PPARα (NR1C1),[1] PPARβ/δ (NR1C2, now described as PPARδ),[2] and PPARγ (NR1C3),[2] regulate the metabolism of fatty acids. Other known specific or nonspecific functions of PPARs include gluconeogenesis, inflammation, and tissue development, repair, and differentiation.[3]

One of the specific functions of PPARδ is tissue repair. Various reports have shown that PPARδ is involved in skin wound healing. For example, the wound healing of skin is reportedly delayed in PPARδ mutant mice (PPARδ^{+/−}),[4] and PPARδ reportedly plays an anti-apoptotic role via the up-regulation of integrin-linked kinase and phosphoinositide-dependent kinase 1[5,6] and ceramide kinase[7] and induces the terminal differentiation of keratinocytes.[8] Moreover, the topical application of a PPARδ agonist has improved the function of a dysfunctional permeability barrier in the skin of hairless mice *in vivo*,[9] and the involvement of PPARδ in the permeability barrier of skin has also been demonstrated using PPARδ^{−/−} mice.[10] Furthermore, PPARδ reportedly modulates the migration and directional sensing of keratinocytes.[11] Thus, ligand activation of PPARδ might promote skin wound healing and help maintain the normal condition of the skin. In fact, the promotion of skin wound healing in mice by administrations of a PPARδ agonist has also been reported.[12]

The initial phase of wound healing in skin is inflammation at the wounded area. PPARδ is up-regulated in keratinocytes via a stress-associated kinase cascade when it is exposed to inflammatory cytokines.[13] In addition, the up-regulation of PPARδ is also reported in mice skin

583

during the wound-healing processes and the expression of PPARδ then gradually decreases to the level found before wound generation, thus suggesting temporal up-regulation in the wound-healing process.[4] Although the anti-inflammatory effect of ligand activation of PPARδ has yet to be elucidated, it has been theorized that, in murine keratinocytes, the inflammatory environment is needed for functional PPARδ and that the cytokine-induced apoptosis is inhibited by the treatment with a PPARδ agonist.[13]

Because the corneal epithelia are located at the outermost layer of corneal tissue, one of their primary functions is protection of the eye from the invasion of pathogens from the external environment. Therefore, corneal epithelia are easily wounded because of trauma, exposure to environmental changes, invasion by pathogenic agents, and major diseases of the cornea. Many previous studies have been conducted to evaluate the promoting effect of compounds on corneal epithelial wound healing. In those reports, a wide variety of mechanisms have been proposed to promote corneal epithelial wound healing: inhibiting inflammation,[14–16] normalizing the condition of tear fluids,[17–19] improving the migration and viability of corneal epithelial cells,[20–23] and regenerating injured corneal nerves or supplying a neurotransmitter.[24,25] However, to our knowledge, there have been no reports aimed at elucidating the function of PPARδ in the corneal epithelium.

In the present study, we evaluated, for the first time to our knowledge, the involvement of PPARδ in corneal epithelial wound healing and the effect of a PPARδ agonist on corneal epithelial wound healing, using cultured cells, experimental animals, and clinical human corneoscleral or corneal specimens.

Materials and Methods

Mechanical Corneal Epithelial Wound Model

All animals used in the experiments were handled in accordance with The Guiding Principles in the Care and Use of Animals (Department of Health, Education, & Welfare publication NIH 80-23) and the Association for Research in Vision and Ophthalmology Statement for the Use of Animals in Ophthalmic and Vision Research. This research was also approved by the ethics committee on human samples of Senju Pharmaceutical Co, Ltd (Kobe, Japan), and adhered to the tenets of the Declaration of Helsinki.

Eighteen male Sprague-Dawley rats, aged 5 weeks (Charles River Laboratories Japan, Kanagawa, Japan), were anesthetized by i.p. injection of 2% sodium pentobarbital (Nacalai Tesque, Kyoto, Japan) at a dosage of 0.2 mL/100 g of body weight. The rat eyes were locally anesthetized by topical administration of 0.4% oxybuprocaine hydrochloride (Santen Pharmaceutical, Osaka, Japan), and then the eyes were exposed from their orbits. The corneal epithelia on the exposed eyes were marked by 3-mm-diameter circles with a trephine blade, and the corneal epithelia inside of the marked circles were then surgically removed by using a commercially available

hand-held diamond-tipped glass engraver (IH-640; Ito Co, Ltd, Hyogo, Japan). General anesthesia was only used during the generation of the wounds, and the animals were awakened after the surgical procedures. In 3 of the 18 animals, the corneal epithelial wound-healing processes were then imaged under a slit-lamp biomicroscope (SL 130; Carl Zeiss, Oberkochen, Germany) with a blue filter after staining of their wounds by topical administration of 5 μL of 0.1% sodium fluorescein solution. The other 15 animals were then euthanized and prepared for immunofluorescent microscopy of their corneas for PPARδ before surgical ablation and at immediately, 8 or 24 hours, or 3 or 7 days after surgical ablation (n = 3 at each time point; samples assigned for before and immediately after surgical ablation were collected from both eyes of the same animals), and the eye tissues were fixed with 10% formalin neutral buffer solution (Wako Pure Chemical, Osaka, Japan) overnight at room temperature.

Effect of a PPARδ Agonist on a Corneal Epithelial Wound-Healing Model

Four male Japanese white rabbits (Kitayama Labes Co, Ltd, Nagano, Japan), weighing approximately 2 kg each, were anesthetized by intramuscular injection of a mixture containing equal volumes of 2% xylazine (Bayer, Osaka, Japan) and 5% ketamine hydrochloride (Sankyo, Tokyo, Japan) at a dosage of 1 mL/kg of body weight. The rabbit eyes were anesthetized locally by the topical administration of 0.4% oxybuprocaine hydrochloride and then exposed from their orbits. The corneal epithelia on the exposed eyes were marked with a 7-mm-diameter circle by using a trephine blade, and the corneal epithelia inside of the marked circles were then mechanically removed by using the previously mentioned commercially available hand-held diamond-tipped glass engraver. General anesthesia was only used during the generation of the wounds, and the animals were awakened after the surgical procedures. When the generation of the wounds had completed, 50 μL of an ophthalmic vehicle solution (PBS; Invitrogen Corporation, Carlsbad, CA) containing 0.1% polysorbate 80 or 1.1 mmol/L GW501516 (0.05% GW501516; Alexis Biochemicals, Lausanne, Switzerland) was topically administrated via micropipettes onto the wounded ocular surfaces of each animal. On the day of wound generation, the animals received two topical administrations of the ophthalmic solution, and on the following day (the final day of evaluation), the animals received four topical administrations of that same solution. The wound areas were then stained with topical administrations of 10 μL of 0.1% sodium fluorescein solution and examined and photographed at 0, 24, 38, and 48 hours after wound generation using a slit-lamp biomicroscope (SL-7F; Topcon, Tokyo, Japan) with a blue filter. The wounded areas shown in the photographs were then measured by using image analyzing software (Image-Pro Plus; Nippon Roper, Tokyo, Japan), and the percentage rates of the remaining wound areas calculated from the initial wound areas [(remaining wound

area/initial wound area) × 100] were used for the evaluation (N = 4 in each group).

Alkali-Induced Keratitis

Forty-five male Sprague-Dawley rats, aged 4 weeks (Charles River Laboratories Japan), were anesthetized generally and topically, and the eyes were then exposed from their orbits by using the same method previously described. Paper filters (3 mm diameter) soaked in 1N NaOH were attached to the center of each corneal surface for 1 minute to remove corneal epithelia and to produce inflammation of the ocular surface, and then the filter papers were removed. After the remaining corneal epithelia were manually removed with a scraper, the ocular surfaces were then washed with saline and the eyes were repositioned into their respective orbits. The corneal epithelial wound-healing processes in 3 of the 45 animals were imaged under a slit-lamp biomicroscope (SL 130) with a blue filter after staining of their wounds by the topical administration of 0.1% sodium fluorescein solution. General anesthesia was only used during the generation of the wounds, and the animals were awakened after the surgical procedures. Of the remaining 42 animals, 21 were then euthanized before receiving the alkali attachment and at immediately, 8 or 24 hours, 3 or 7 days, or 3 weeks after receiving the alkali attachment. The eye balls of those 21 animals were then enucleated and embedded in optimal cutting temperature (OCT) compound (Tissue-Tek; Sakura Finetek Japan Co, Ltd, Tokyo, Japan) for preparation of the frozen sections (n = 3 at each time point).

Ex Vivo Human Corneal Epithelial Wound Model

Residual portions of healthy human corneoscleral tissue obtained during corneal transplantation were obtained from the Northwest Lion Eye Bank (Seattle, WA) for use in this study. Those residual portions were stored for 4 to 5 days at 4°C in Optisol-GS (Bausch & Lomb, Rochester, NY) corneal preservation medium until immediately before use. The epithelia of those residual portions were surgically abraded, cut radially with a knife, and then incubated in Optisol-GS at 37°C in an environment of 5% CO_2, 95% air, and 100% humidity. The tissues were collected before receiving the ablation and at immediately or at 24 or 48 hours after receiving the ablation, embedded in Tissue-Tek OCT compound, and then frozen for preparation of the frozen sections. Additional tissues that did not undergo epithelial ablation were incubated for 24 hours in the absence or presence of 10 ng/mL tumor necrosis factor (TNF)-α (R&D Systems Inc., Minneapolis, MN), because it induces up-regulation of PPARδ and apoptosis in keratinocytes,[13] and then frozen in Tissue-Tek OCT compound (n = at least 2 at each time point).

Immunofluorescent Microscopy

For immunofluorescent microscopy of the rat eyes, the tissues fixed with 10% formalin solution were paraffinized, embedded in paraffin, and then cut into sections (6-μm-thick specimens) by using a microtome. These specimens were deparaffinized by a double immersion in xylene and a single immersion in 100%, 99.5%, 95%, 90%, and 70% ethanol, and they were then immersed in water and washed with PBS. For immunofluorescent microscopy of the human corneoscleral tissues, the tissues were embedded in Tissue-Tek OCT compound, frozen, and then cut into sections (6-μm-thick specimens) by using a cryostat. The sectioned specimens were then fixed with 10% formalin neutral buffer solution at 4°C for 15 minutes and washed three times with PBS. For immunofluorescent microscopy of the human corneal epithelial cells (HCECs), the cultured cells were fixed in cold methanol (−30°C) for 5 minutes, air dried, and then washed three times with PBS. The specimens were then blocked with 10% normal blocking serum samples (Millipore, Billerica, MA), which were derived from the same species in which the secondary antibodies were raised, for 20 minutes at room temperature. The specimens were then labeled with 4 μg/mL of primary antibodies containing 1.5% normal blocking serum samples for 1 hour at room temperature. They were then washed three times with PBS and labeled with fluorochrome-conjugated secondary antibodies (Alexa Fluor IgGs; Molecular Probes, Eugene, OR) at 10 μg/mL concentrations containing 3% normal blocking serum samples for 45 minutes at room temperature. They were then washed three times with PBS and mounted with Vectashield (Vector Laboratories, Burlingame, CA) containing 0.5% DAPI (Dojindo, Kumamoto, Japan). For staining of PPARδ in the rat specimens, we used donkey serum for the normal blocking serum, anti-PPARδ goat IgG (sc-1987; Santa Cruz Biotechnology, Inc., Santa Cruz, CA) for the primary antibody, and Alexa Fluor 488 donkey anti-goat IgG. For staining of PPARδ in the human specimens, we used goat serum for the normal blocking serum, anti-PPARδ rabbit IgG (sc-7197; Santa Cruz Biotechnology) for the primary antibody, and Alexa Fluor 488 goat anti-rabbit IgG. For staining of IL-1β in the rat specimens, we used goat serum for the normal blocking serum, anti-IL-1β rabbit IgG (BS3506; Bioworld Technology, Inc., Minneapolis, MN) for the primary antibody, and Alexa Fluor 568 goat anti-rabbit IgG. The stained specimens were then observed by using a laser confocal microscope (FV-1000; Olympus, Tokyo, Japan).

TUNEL Staining

Eye tissues obtained from the rats and humans were embedded in Tissue-Tek OCT compound, frozen, and then cut into sections (6-μm-thick specimens) by using a cryostat. DNA fragmentations of those tissues were detected by TUNEL staining using an In Situ Cell Death Detection Kit (Fluorescein; Roche Diagnostics Corp, Indianapolis, IN), according to the manufacturer's protocol.

The stained specimens were then observed with a laser confocal microscope.

Annexin V–Propidium Iodide Staining

Human corneoscleral tissues that had received surgical ablation of their corneal epithelia were pretreated with the PPARδ agonist GW501516 (EC_{50} = 1.1 nmol/L) and/or a PPARδ antagonist GSK0660 (IC_{50} = 155 nmol/L; Sigma-Aldrich, St. Louis, MO) for 2 hours at 37°C in an environment of 5% CO_2, 95% air, and 100% humidity. The specimens were then further incubated with stimulation by TNF-α (20 ng/mL) for 24 hours at 37°C in the same environment. After incubation, cell death in those specimens was detected by using the Annexin V-FLUOS Staining Kit (Roche Diagnostics), which can detect annexin V and staining with propidium iodide, according to the manufacturer's protocol. The stained specimens were then observed with a laser confocal microscope.

Quantifications of Cytokines

The corneas of the 21 animals that were collected before receiving alkali attachment and at immediately, 8 or 24 hours, 3 or 7 days, or 3 weeks after receiving alkali attachment were frozen with liquid nitrogen and crushed by using a cryopress. Then, the cellular lysate was prepared for cytokine quantification using a lysis buffer consisting of a radioimmunoprecipitation assay (Sigma-Aldrich) supplemented with protease inhibitors (Protease Inhibitor Cocktail Tablets, complete, Mini; Roche Diagnostics). Then, IL-1β and TNF-α in each lysate were quantified using Quantikine Rat TNF-α/TNFSF1A Immunoassay and Quantikine Rat IL-1β/IL-1F2 Immunoassay (R&D Systems), respectively, according to the manufacturer's protocol (n = 3).

Cell Cultures

RbCEC Findings

Rabbit corneal epithelial cells (RbCECs) were prepared and cultured according to the previously reported method.[26] In brief, the corneas were enucleated from euthanized male Japanese white rabbits weighing approximately 1.5 kg each (Kitayama Labes), and the endothelial layers of those corneas were then mechanically removed by gently scraping a surgical knife (Alcon Laboratories, Inc., Fort Worth, TX) until the layers could be observed to be peeling from the cornea. The remaining corneal tissues were transferred to minimum essential medium (Invitrogen) containing dispase II (Roche Diagnostics) at 2.4 U/mL and then incubated at 37°C for 1 hour. The corneal epithelia were then peeled and further incubated with trypsin-EDTA (Invitrogen) at 37°C for 5 minutes to dissociate adhesion between the cells. The prepared RbCECs were seeded into a culture dish using rabbit corneal growth medium 2 (Kurabo Industries, Osaka, Japan). The RbCECs were then cultured at 37°C with 5% CO_2, and the medium was exchanged with fresh medium every 48 hours until the cells reached subconfluence.

HCEC Findings

The HCECs, proprietary medium for the cell culture (EpiLife; Kurabo Industries), and the supplements to maintain cell proliferation [an HCGS (Human Corneal Growth Supplement) proliferation additive set containing insulin, hydrocortisone, transferrin, epidermal growth factor (EGF), and bovine pituitary extract] were obtained from Kurabo Industries. Two kinds of media were prepared and used [ie, complete EpiLife, which contained all five supplements to maintain the cell culture; and basal EpiLife, which contained three supplements (insulin, hydrocortisone, and transferrin) to assay the cells' DNA fragmentation, lactate dehydrogenase (LDH) release, and proliferation]. Basal EpiLife was used for limiting and synchronizing the cells' growth, because the purpose of some of the experiments using HCECs was to evaluate cell death and proliferation. HCECs were seeded into a culture dish using complete EpiLife. The HCECs were then cultured at 37°C in 5% CO_2, with the medium being exchanged with fresh complete EpiLife every 48 hours until the cells reached subconfluence.

RT-PCR Data

Total RNAs were extracted from the RbCECs, rabbit corneal epithelia collected before their ablation, HCECs, and human corneal epithelia separately isolated from their center region and limbus by TRIzol reagent (Invitrogen), according to the manufacturer's protocol. For RT-PCR, preparations of cDNAs from the extracted total RNAs were obtained according to the manufacturer's protocol (Superscript II Reverse Transcriptase; Invitrogen). The RT reaction mixture consisted of 10 ng/mL DNase-treated RNA, one times first-strand buffer, 1 U/μL RNase inhibitor (SUPERNase-In; Applied Biosystems/Ambion, Austin, TX), 10 mmol/L dithiothreitol, 500 μmol/L each deoxyribonucleotide triphosphate, and 25 ng/μL random primers (Invitrogen); these were incubated at 25°C for 10 minutes, 42°C for 50 minutes, and 70°C for 15 minutes. A PCR of the PPAR genes and glyceraldehyde-3-phosphate dehydrogenase was performed with the Platinum Blue PCR SuperMix (Invitrogen), according to the manufacturer's protocol. PPAR and glyceraldehyde-3-phosphate dehydrogenase primers were designed so that the PCR product became approximately 200 bp, in reference to the known sequences of humans, chimpanzees, crab-eating macaques, cattle, and mice. The primers were set as follows: PPARα, 5'-GTAGAATCTGCGGGGACAAG-3' (forward) and 5'-GTTGTGTGACATCCCGACAG-3' (reverse); PPARδ, 5'-TTCCTTCCAGCAGCTACACA-3' (forward) and 5'-GATCGTACGACGGAAGAAGC-3' (reverse); and PPARγ, 5'-GATGCAGGCTCCACTTTGAT-3' (forward) and 5'-CTCCGTGGATCTCTCCGTAA-3' (reverse). All of these primers were designed as having intron-overlapping sequences. The PCR was performed for 35 cycles at 94°C for 30 seconds, at 55°C for 30 seconds, and at 72°C for 30 minutes. The PCR products were applied to electrophoresis using 2% agarose gels, and then the DNA samples separated in the gels were

stained with SYBR Gold (Molecular Probes) dye and visualized under a UV transilluminator.

In Vitro *Wound Closure Assay*

For an *in vitro* wound closure assay, HCECs were seeded into culture flasks using complete EpiLife culture medium and cultured at 37°C in 5% CO_2 until the cells reached subconfluence. The medium was then exchanged with basal EpiLife culture medium, and the HCECs were cultured for an additional 24 hours. Next, the cells received a treatment of small-interfering RNA (siRNA) transfection according to the manufacturer's protocol. Briefly, the cells were harvested from the culture flasks and then transferred into experimental wells containing complexes consisting of 4 μL of one of three siRNAs (ie, PPARD Silencer Select Validated siRNA, IDs S10883 and S10884; and Silencer Select Negative Control 1 siRNA; Applied Biosystems/Ambion) and 1 μL of transfection agent (siPORT NeoFX Transfection Agent; Applied Biosystems/Ambion) per well, for transfecting siRNAs to the cells using basal EpiLife. The transfected cells were seeded onto a 48-well cell culture plate (BD Falcon, Franklin Lakes, NJ), in which a 7-mm-diameter circular seal was affixed to the bottom of each well, and then cultured for 24 hours. After attachment of the cells onto the bottom of the experimental wells by 24 hours of culture, the cells were incubated with or without 1 nmol/L of GW501516 for 2 hours, and then the affixed seals were removed from the bottom of each well to generate cell-free areas of the same size (experimental *in vitro* wound). The cells were then cultured for an additional 48 hours. After the 48 hours of culture, the plates were washed two times using Dulbecco's PBS and the cells were fixed with 10% formalin neutral buffer solution for 15 minutes at room temperature. The fixed cells were then washed three times using Dulbecco's PBS and stained with 0.05% toluidine blue solution (Wako Pure Chemical). The bottom of each of the stained experimental wells was then photographed, and the no-stained area, where the cells were absent, was measured by using imaging software (Image-Pro Plus) as a nonhealed area.

For assaying PPARδ gene expression, total RNAs from the cells that received siRNA transfection treatments in a method similar to the *in vitro* wound closure assay previously described were prepared by using the RNeasy Mini Kit (Qiagen, Hilden, Germany), according to the manufacturer's protocol, and their cDNAs were then prepared from the extracted total RNAs, according to the previously mentioned protocol. Then, *PPARδ* and *GAPDH* genes were assayed by using their specific TaqMan Gene Expression Assays (Applied Biosystems/Ambion) and TaqMan Gene Expression Master Mix (Applied Biosystems/Ambion), according to the manufacturer's protocol, with the 7500 Real-Time PCR System (Applied Biosystems/Ambion).

Western Blot Analyses

For preparation of the HCEC lysates, the cells were seeded into culture dishes using complete EpiLife culture medium and cultured at 37°C in 5% CO_2 until the cells

reached subconfluence. Then, the medium was exchanged with basal EpiLife culture medium and the HCECs were cultured for 24 hours. The cells were further cultured with or without pretreatment with a PPARδ agonist (GW501516) or an antagonist (GSK0660) for 2 hours, and then for 24 hours using basal EpiLife in the absence or presence of the following cytokines: 100 ng/mL TNF-α and 10 ng/mL interferon (IFN)-γ (R&D Systems). The HCECs were then washed two times using ice-cold Dulbecco's PBS (Invitrogen) and then lysed in the previously described cold lysis buffer. Insoluble materials contained within those lysates were then removed by centrifugation at 10,000 $\times$ g for 10 minutes at 4°C, and protein concentrations in the collected supernatants were quantified by using the BCA Protein Assay Kit (Thermo Fisher Scientific, Inc., Waltham, MA). Equal amounts of those soluble proteins were separated using SDS-PAGE, and they were then transferred onto a polyvinylidene difluoride membrane. After 1-hour blocking in 5% nonfat dry milk in Tris-buffered saline with 0.1% Tween-20, the membranes were incubated in a primary antibody against PPARδ (sc-74440; Santa Cruz Biotechnology). Visualization of PPARδ was performed by using horseradish peroxidase–conjugated goat anti-mouse IgG (Santa Cruz Biotechnology) as a secondary antibody and enzyme-linked chemiluminescence (Thermo Fisher Scientific). After performing Western blot analysis for PPARδ, the conjugated antibodies were removed by using a stripping solution (WB Stripping Solution Strong; Nacalai Tesque) and the same membranes were used for detection of β-actin. For the visualization of β-actin, a primary antibody against β-actin (sc-47778; Santa Cruz Biotechnology) and horseradish peroxidase–conjugated goat anti-mouse IgG were used. The concentrations of visualized PPARδ and β-actin bands were measured by software (Image-Pro Plus), and the quantities of PPARδ bands were compared after the revisions using the quantities of β-actin bands: PPARδ/β-actin band on the same membrane ($n = 2$ in each group). Western blot analysis for poly ADP ribose polymerase (PARP) was demonstrated as previously described, except for using a primary antibody against PARP (AM30; Merck KGaA, Darmstadt, Germany).

Cell Viability Assay

HCECs were seeded into 225-cm^2 culture flasks using complete EpiLife and then cultured at 37°C in an environment of 5% CO_2, 95% air, and 100% humidity until the cells reached subconfluence. When the HCECs reached subconfluence, they were seeded into 96-well culture plates using complete EpiLife and were cultured for 48 hours. Then, the medium was exchanged with basal EpiLife and the cells were cultured for an additional 24 hours. After pretreatment of those cells with GW501516 for 2 hours, the cells were cultured for 24 hours in the absence or presence of the following cytokines: 100 ng/mL TNF-α and 10 ng/mL IFN-γ. After the 2- and 24-hour stimulation with the PPARδ agonist and the cytokines, respectively, the cells were seeded into 96-well culture plates for evaluations of their DNA fragmentations and incorporations of 5-bromo-2'-deoxyuridine (BrdU) us-
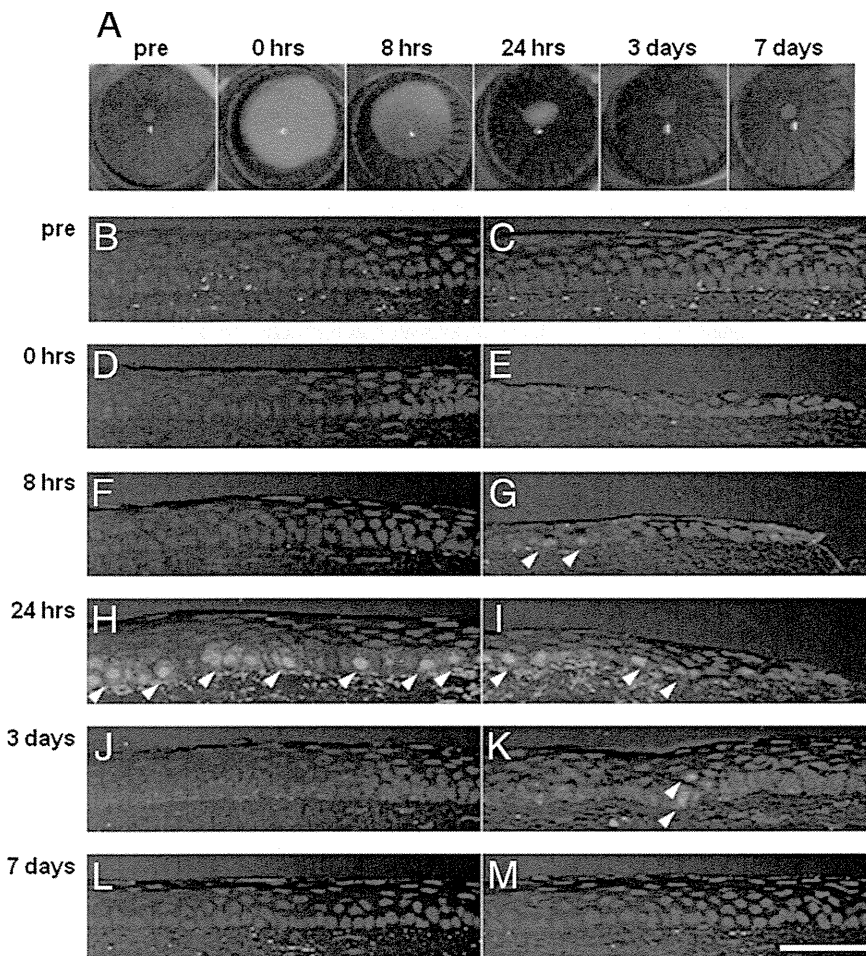
Figure 1. Protein expression of PPARδ in the rat corneal epithelia during wound healing. **A:** Representative photographs of the rats' ocular surfaces during corneal epithelial wound healing. Green areas represent fluorescein-stained areas of the corneal epithelial wounds. The wounds became increasingly smaller for up to 24 hours after wound generation and had completely healed at 3 days after the generation. **B–M:** Representative photographs of immunofluorescent staining for PPARδ in the rat corneal epithelia during wound healing. **B:** Corneal periphery before wound generation. **C:** Central cornea before wound generation. **D:** Corneal periphery immediately after wound generation. **E:** Edge of the epithelial wound immediately after wound generation. **F:** Corneal periphery at 8 hours after wound generation. **G:** Edge of the epithelial wound at 8 hours after wound generation. **H:** Area next to the epithelial wound edge at 24 hours after wound generation. **I:** Edge of the epithelial wound at 24 hours after wound generation. **J:** Corneal periphery at 3 days after wound generation. **K:** Central cornea at 3 days after wound generation. **L:** Corneal periphery at 7 days after wound generation. **M:** Central cornea at 7 days after wound generation. The blue and green staining represents the cellular nuclei and PPARδ, respectively. Staining of PPARδ is indicated by **white arrowheads (G–I** and **K).** PPARδ was faintly expressed at 8 and 24 hours after wound generation, peaking at 24 hours after wound generation. Scale bar = 50 μm.

ing the Cell Death Detection enzyme-linked immunosorbent assay (ELISA) (Roche Diagnostics) and the Cell Proliferation ELISA, BrdU (colorimetric) (Roche Diagnostics), respectively; their culture media were used for an evaluation of their LDH release using the LDH Cytotoxicity Detection Kit (Takara Bio, Shiga, Japan), according to manufacturers' protocols. The measured value in each culture well was then converted into a percentage when the averaged value of the nontreated group was 100% in each assay (at least 6 in each group of every assay).

Statistical Analyses

Statistical analyses were performed using the SPSS 11.0J data analysis system (SPSS Inc., Tokyo, Japan). The measured data in this study were statistically analyzed by using the Student's t-test, and $P < 0.05$ was considered statistically significant.

Results

Temporal Expression of PPARδ during Corneal Epithelial Wound Healing

Corneal epithelial wounds generated by surgical ablation in the rats were nearly completely healed at 24 hours and were completely healed at 3 days after generation (Figure 1A). During the wound-healing processes, an obvious sign of PPARδ immunostaining was not found on the nucleus of the corneal epithelial cells in the nonabraded corneal tissues or in the corneal tissues collected immediately after the ablations (Figure 1, B–M). Although some fine signals were observed in the corneal epithelia collected before wound generation (Figure 1, B and C), they were judged to be artifacts of the staining because they were observed in corneal epithelia and in the stroma, not corresponding to the cellular nuclei. However, a few faint signs of PPARδ immunostaining on the cell nucleus were observed at the region of the wound's edge of the corneal epithelia collected at 8 hours after the ablations (Figure 1G). In the corneal epithelia collected at 24 hours after the ablations, PPARδ immunostaining was widely observed on the cell nucleus of cells mainly distributed near the wounded region (Figure 1, H and I). Although the remaining few PPARδ-immunostained cell nuclei were observed in the central, just-closed regions of the wounds of the corneal epithelia collected at 3 days after the ablations (Figure 1K), they had completely disappeared at 7 days after the ablations (Figure 1, L and M). The expressions of PPARδ were localized in the corneal epithelial basal cells.
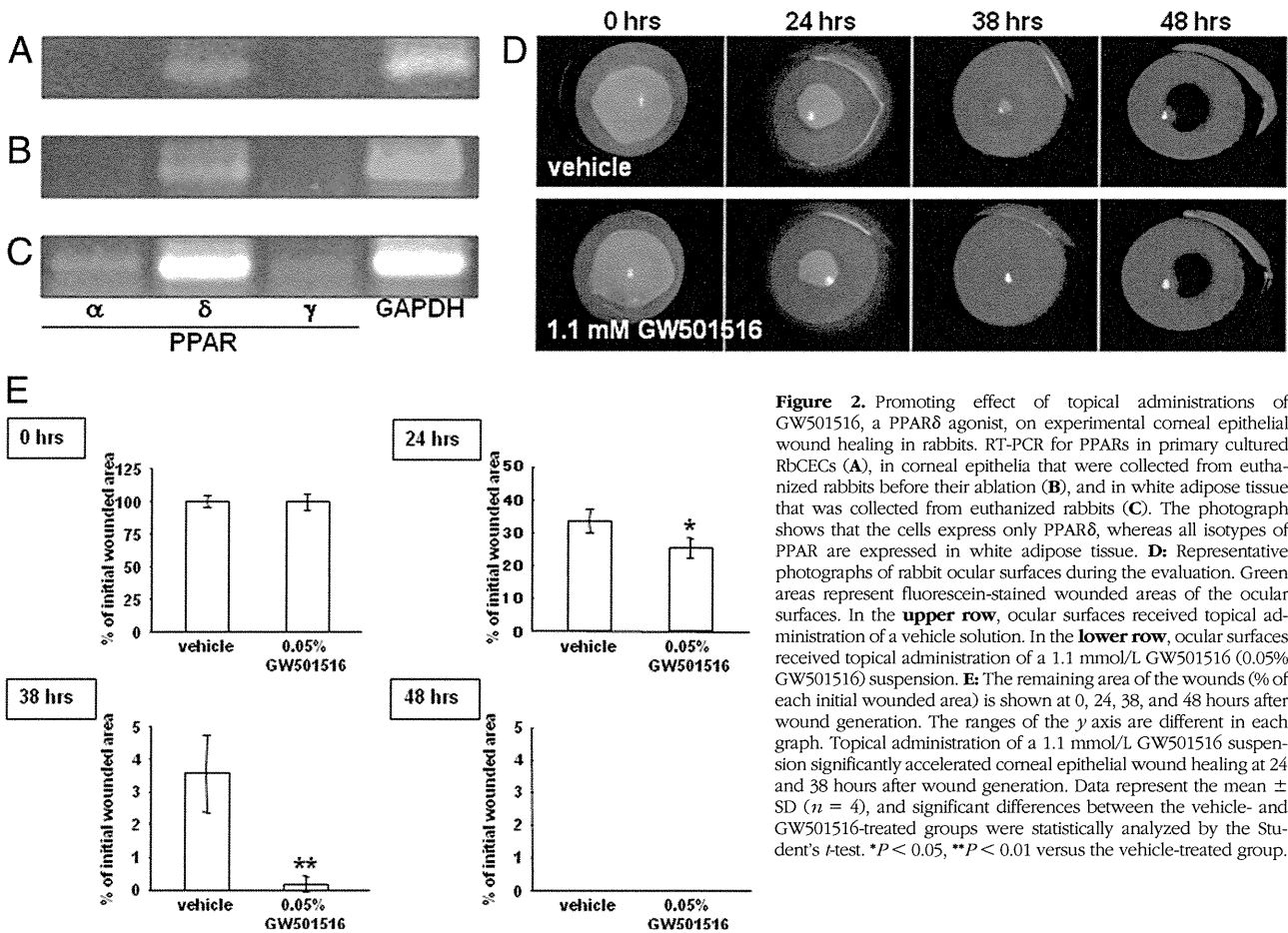
Figure 2. Promoting effect of topical administrations of GW501516, a PPARδ agonist, on experimental corneal epithelial wound healing in rabbits. RT-PCR for PPARs in primary cultured RbCECs (**A**), in corneal epithelia that were collected from euthanized rabbits before their ablation (**B**), and in white adipose tissue that was collected from euthanized rabbits (**C**). The photograph shows that the cells express only PPARδ, whereas all isotypes of PPAR are expressed in white adipose tissue. **D:** Representative photographs of rabbit ocular surfaces during the evaluation. Green areas represent fluorescein-stained wounded areas of the ocular surfaces. In the **upper row**, ocular surfaces received topical administration of a vehicle solution. In the **lower row**, ocular surfaces received topical administration of a 1.1 mmol/L GW501516 (0.05% GW501516) suspension. **E:** The remaining area of the wounds (% of each initial wounded area) is shown at 0, 24, 38, and 48 hours after wound generation. The ranges of the y axis are different in each graph. Topical administration of a 1.1 mmol/L GW501516 suspension significantly accelerated corneal epithelial wound healing at 24 and 38 hours after wound generation. Data represent the mean ± SD (n = 4), and significant differences between the vehicle- and GW501516-treated groups were statistically analyzed by the Student's t-test. $*P < 0.05$, $**P < 0.01$ versus the vehicle-treated group.

Effect of Topical Administrations of a PPARδ Agonist on Corneal Epithelial Wound Healing

To evaluate the effect of topical administrations of a PPARδ agonist on corneal epithelial wound healing, we first checked the expression of PPAR mRNAs in the rabbit corneal epithelia. Both cultured RbCECs (Figure 2A) and quiescent corneal epithelia that were collected before their ablation from rabbits (Figure 2B) expressed PPARδ mRNA, yet the expression of PPARα and PPARγ mRNAs was not detected in them. On the other hand, all isotypes of PPAR mRNAs were detected in white adipose tissue from rabbits (Figure 2C), demonstrating that the primers could detect PPARα and PPARγ mRNAs from rabbits, if they were expressed. Corneal epithelial wound healing of the wounds generated by surgical ablation in the rabbits significantly accelerated when treated by topical administrations of the PPARδ agonist (GW501516) suspension compared with the wounds that received the topical administration of a vehicle solution alone (Figure 2, D and E), both at 24 and 38 hours after wound generation. We evaluated the effect of another synthetic PPARδ agonist on corneal epithelial wound healing using the previously mentioned experimental model, in which the agonist also promoted the wound-healing processes, showing its dose dependency (data not shown).

Effect of a PPARδ Agonist on an in Vitro Wound Closure System Using HCECs

To demonstrate the specificity of a PPARδ agonist, GW501516, to PPARδ during corneal epithelial wound healing, we next evaluated it using an *in vitro* wound closure system, in which the cells were transfected with siRNAs for PPARδ to inhibit the expression, using HCECs. In cultured HCECs, PPARδ expression was significantly decreased by treatment with either one of two kinds of PPARδ siRNAs (S10883 or S10884), whereas the negative control (NC) siRNA did not show any decrease of the expression (Figure 3A). In this condition, we evaluated the effect of a PPARδ agonist, GW501516, on *in vitro* wound closure by HCECs. When the HCECs did not receive any siRNAs or received treatment of an NC siRNA, GW501516 showed significant promotion of the wound closure. On the other hand, when the cells received treatment of PPARδ siRNAs, in which PPARδ expression decreased, the agonist failed to demonstrate the promoting effect (Figure 3C). In addition, significant delays of the wound closure were also observed in the cells treated with PPARδ siRNAs (Figure 3, B and C). These findings suggested that the effect of a PPARδ agonist, GW501516, on corneal epithelial wound healing must be specifically demonstrated via PPARδ.
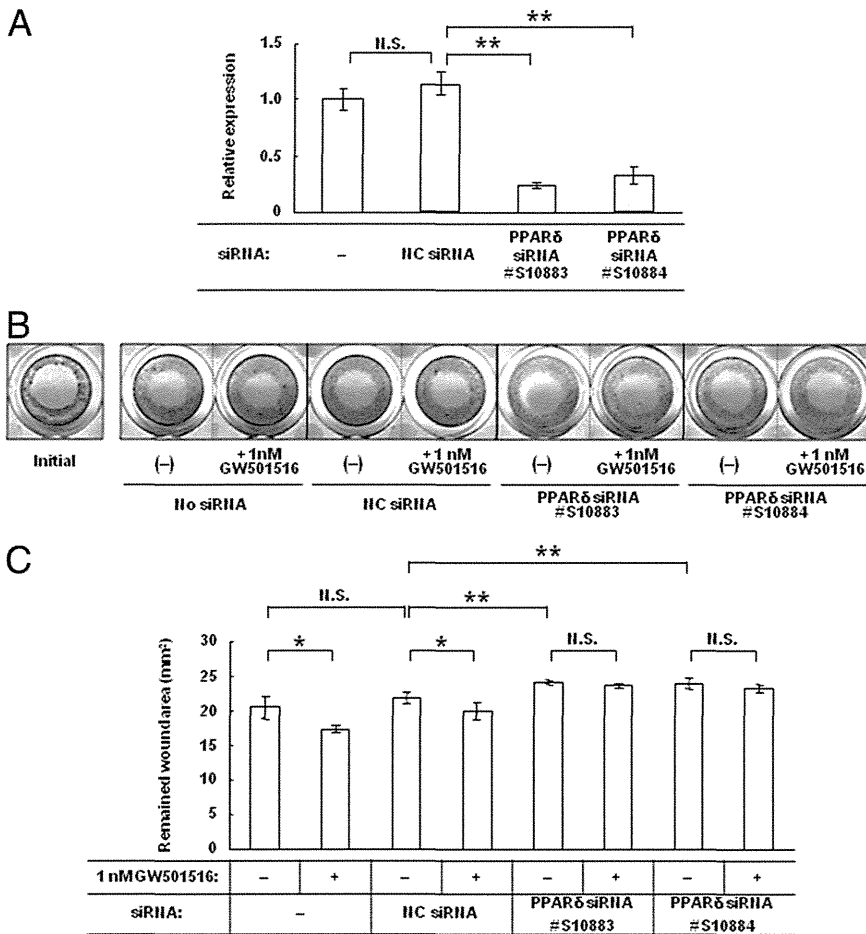
A

B

C

Figure 3. Promoting effect of GW501516, a PPARδ agonist, on *in vitro* corneal epithelial wound closure by HCECs and its specificity to PPARδ using PPARδ siRNAs during the processes. **A:** Real-time PCR for PPARδ shows that treatment of HCECs with siRNAs for PPARδ decreases the expression of PPARδ. Data represent the mean ± SD (*n* = 3 to 4). The significant differences between the no siRNA and NC siRNA treated groups was statistically analyzed by using the Student's *t*-test, in which there were no significant differences (N.S. indicates not significant), and among NC siRNA and PPARδ siRNA, treated groups were analyzed by using the Dunnett's test. **P < 0.01 versus the NC siRNA-treated group. **B:** Representative photographs of experimental wells, in which stained HCECs are violet. Initial means the cells were stained immediately after the experimental wounds' generation. Pretreatment with a PPARδ agonist of the cells shows 1 nmol/L GW501516 or (-), which indicates no pretreatment. The transfected siRNAs are indicated as No siRNA, NC siRNA, PPARδ siRNA S10883, or PPARδ siRNA S10884. **C:** A graph showing each remaining wound area at 48 hours after wound generation. Data represent the mean ± SD (*n* = 4). The significant differences between the no siRNA and NC siRNA treated groups were statistically analyzed by using the Student's *t*-test, in which there were no significant differences, and those among NC siRNA and PPARδ siRNA treated groups were analyzed by using the Dunnett's test. **P < 0.01 versus the NC siRNA treated group. The promoting effect of GW501516 on the wound closure processes was statistically analyzed by using the Student's *t*-test between groups that received the same siRNA treatments. *P < 0.05.

Effect of a PPARδ Agonist on Inflammation-Induced HCEC Apoptosis

To elucidate the underlying mechanisms by which a PPARδ agonist promotes wound healing in corneal epithelia, we evaluated the effect of the PPARδ agonist, GW501516, on apoptosis, necrosis, and proliferation of cultured HCECs, which expressed all three PPAR mRNAs (Figure 4A). We theorize that the reason why the expression pattern of the isotype in the HCECs was not the same pattern as that observed in RbCECs (Figure 2, A and B) may be due to the differences between the species and the different function of those isotypes during corneal epithelial wound-healing processes among animal species. Because of the fact that the corneal epithelial wound-healing process at the ocular surface sometimes coincides with inflammation in both rat and rabbit experimental models *in vivo*, the cells were treated with cytokines (100 ng/mL TNF-α plus 10 ng/mL IFN-γ) to cause changes in cell viability. The treatment with cytokines caused an up-regulation of the PPARδ protein in the HCECs (Figure 4B), and this up-regulation agreed with the previous results observed in rats by using immunofluorescent microscopy (Figure 1, B–L). Moreover, the treatment with cytokines caused statistically significant increases of DNA fragmentation (Figure 5A) and LDH release (Figure 5C), as well as a decrease of BrdU incor-

poration (Figure 5D), in the HCECs. In these assay systems, treatment of the cells with camptothecin, a well-known topoisomerase I inhibitor and apoptosis inducer, produced a marked increase of DNA fragmentation (Figure 5A) and LDH release (Figure 5C), suggesting that the inhibitor caused apoptosis and necrosis of the cells. On the other hand, treatment of the cells with brain and reproductive organ-expressed (BRE) and EGF caused an obvious increase of BrdU incorporation (Figure 5D), suggesting that the supplemental treatment with BRE and EGF increased the proliferative activity of the cells.

In the previously mentioned assay systems, the PPARδ agonist, GW501516, caused a statistically significant inhibitory effect on the DNA fragmentation in the HCECs induced by treatment with cytokines (Figure 5A), suggesting that PPARδ agonists produce an anti-apoptotic effect. Although the effective concentrations of GW501516 in this study were low (1 nmol/L) compared with those in other reports, the EC_{50} value used in this study is similar to that used in the previous reports (1.1 nmol/L).[27] On the other hand, in the absence of cytokines, the DNA fragmentation (apoptosis) was induced by the treatment with GW501516 (Figure 5A).

We believe that these contrary effects are interesting because they suggest the function of PPARδ agonists on corneal epithelial cells. We hypothesize that PPARδ ago-
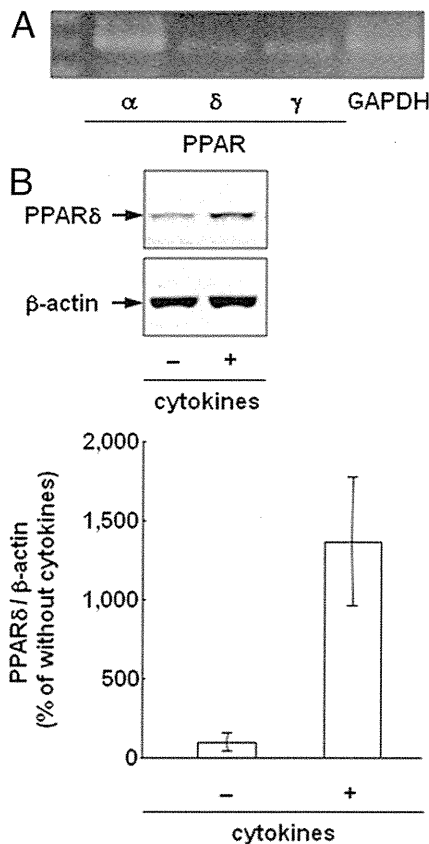
Figure 4. A: RT-PCR for PPARs in healthy HCECs. The human-derived cells expressed all PPARs: α, δ, and γ. GAPDH indicates glyceraldehyde-3-phosphate dehydrogenase. **B:** Western blot analysis for PPARδ as a target and β-actin as an internal standard. The results of the analyses show that the protein levels of PPARδ are up-regulated in the cells by treatment with cytokines (100 ng/mL TNF-α and 10 ng/mL IFN-γ). Data from Western blot analyses are represented as mean ± SD ($n = 2$).

pounds did not change the number of corneal cells when the animals did not receive corneal epithelial wounds (Y. Nakamura, unpublished data).

Furthermore, we also evaluated the effect of a PPARδ agonist/antagonist on early apoptosis in HCECs by using Western blot analysis for PARP, whose degradation suggests early apoptosis with activation of caspase. As a result, we observed that stimulation of the cells by cytokines induced marked degradation of PARP showing caspase activation and early apoptosis, but the degradation was inhibited by neither the agonist nor the antagonist (Figure 5B). These results suggest that PPARδ may
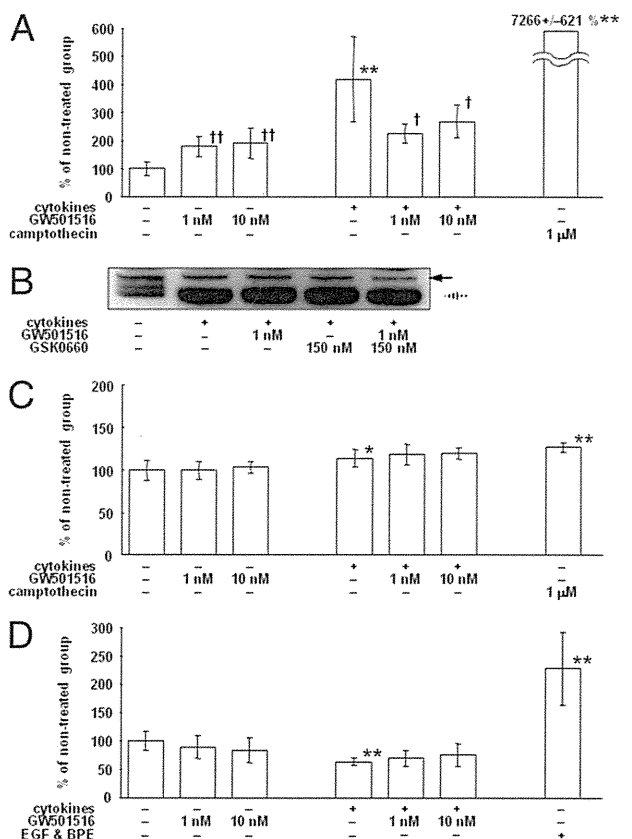

Figure 5. The effect of GW501516 on cytokine-induced DNA fragmentation (**A**), a representative photograph of Western blot analysis for PARP (**B**), LDH release (**C**), and decrease of BrdU incorporation (**D**), in healthy HCECs. In **A**, **C**, and **D**, levels are represented as a percentage of the nontreated group. Data in these three graphs are represented as mean ± SD ($n = 12$ for the nontreated group and the EGF- and bovine pituitary extract–treated groups, and $n = 6$ for the other groups), and significant differences between the nontreated group and the cytokine-treated group or each positive control group (1 μmol/L camptothecin-treated group for DNA fragmentation assay and LDH activity assay, and EGF- and bovine pituitary extract–treated group for BrdU incorporation assay) were statistically analyzed by the Student's t-test (*$P < 0.05$, **$P < 0.01$ versus the nontreated group). Significant differences between the nontreated group and GW501516-treated groups and between the cytokine-treated group and the cytokine plus GW501516-treated groups were analyzed by the Dunnett's test (††$P < 0.01$ versus the nontreated group, and †$P < 0.05$ versus the cytokine-treated group, respectively). In photographs of Western blot analysis for PARP (**B**), the **solid arrow** and the **dashed arrow** show intact PARP and degraded PARP, respectively. The photograph represents the result in three differently repeated experiments. Data show the degradation of PARP in cultured HCECs treated with cytokines and no effects of the PPARδ agonist/antagonist on the degradation.
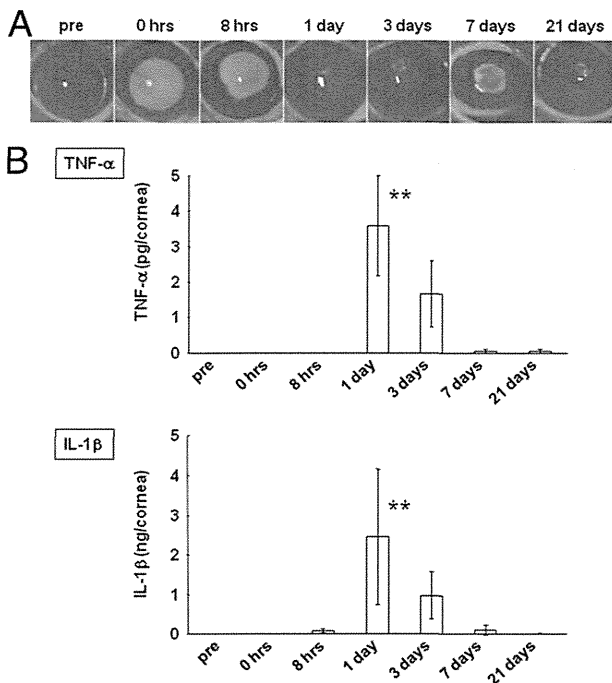
nists may inhibit epithelial cell death when the cell death is ongoing; however, that cell death may be induced during active cell growth. In other words, PPARδ might have a function in maintaining the number of corneal epithelial cells. In fact, previously published studies have already demonstrated this contradiction. For example, one study[4] reported the anti-apoptotic effects of PPARδ, whereas another study[28] reported no anti-apoptotic effect and no proliferative effects of the receptor; a third study[29] reported the proliferative effects of the receptor. The findings of those studies have been reviewed in a separate publication,[30] in which the authors mention that those contradictory findings may be the result of the different experimental strategies used in the three previously referenced studies. In addition, they hypothesize that, although PPARδ affects the expression of inducers and inhibitors of cell proliferation, this receptor is not a bona fide cell cycle regulator with a defined function.[30] Our findings showed a novelty that a PPARδ agonist demonstrated such antithetic effects, even in a single evaluation system, one in which corneal epithelial cells were used. We are in the process of investigating this hypothesis. For example, although topical administrations of PPARδ agonists showed a promoting effect on corneal epithelial wound healing in rabbits, these com-

Figure 6. Analyses of the wound-healing process in rat corneas with alkali-induced keratitis. **A:** Representative photographs of rat ocular surfaces during corneal epithelial wound healing after receiving alkali attachment. Bright green areas represent fluorescein-stained areas of the corneal epithelial wounds. The wounds had healed by 1 to 3 days after injury, but recurrence of the wounds was observed in two of the three injured eyes. **B:** Protein expression changes of pro-inflammatory cytokines in corneas that received alkali-induced keratitis. Cytokines were measured by ELISA. **Top** and **bottom:** The levels of TNF-α and IL-1β, respectively. Data are represented as mean $\pm$ SD ($n = 3$), and significant differences in the corneal cytokine levels at each time point between the alkali attachment group and the nontreated group (pre) were statistically analyzed by the Dunnett's test. **$P < 0.01$ versus the nontreated group.

not be affected in early apoptosis, at least not in our experiment.

In contrast to the results of the DNA fragmentation assay, GW501516 did not affect the LDH release from HCECs or the BrdU incorporation into those cells using the culture media, both in the absence and in the presence of cytokines, thus indicating that it is impossible for PPARδ agonists to inhibit cell necrosis, or promote cell proliferation, *in vitro*.

Sustained Expression of PPARδ and Corneal Epithelial Cell Death in Alkali-Induced Keratitis

Next, the investigation was focused on whether much inflammation at the ocular surface caused up-regulation of the PPARδ protein and the death of corneal epithelial cells. For this investigation, an alkali-induced keratitis rat model was used to observe healing processes of corneal epithelial wounds induced by alkali attachment; in some cases of this experimental keratitis model, we also observed their recurrence (Figure 6A). During those processes of this experimental keratitis, measurement by ELISA showed that the protein levels of cytokines TNF-α and IL-1β temporally increased in the rat corneas, with that increase peaking at 1 day after alkali attachment, and that the IL-1β level was much higher than the TNF-α

level (Figure 6B). Although these data showed wide variances because the degree of corneal inflammation might be different among the animals, a statistically significant increase of corneal cytokines was observed at 1 day after their receipt of alkali attachment. The up-regulation of IL-1β was also observed by immunofluorescent microscopy. IL-1β staining of the cell nucleus was detected at 8 hours and at 1, 3, and 7 days after alkali attachment, and the signals were widely distributed throughout the corneal epithelia, thus showing an intense and temporal inflammatory response to alkali attachment (Figure 7, A–G). In addition, we assayed those cytokines secreted from isolated corneas, which had received alkali attachments before their enucleation, to their cultured media using an *ex vivo* tissue culture system to confirm that those cytokines were secreted from corneal epithelial cells that received alkali attachment. As a result, a significant increase of cytokines could not be observed (data not shown), although increases of cytokines in corneal epithelial cells had been observed after alkali attachment (Figure 7, A–G), thus supporting the ELISA data (Figure 6B). This difference may be explained by corneal inflammation increasing by interactions between corneal cells and other types of cells (eg, neutrophils),[31] whereas the infiltrations of kinds of inflammatory cells into the cornea were not permitted in this assay using an *ex vivo* system. Therefore, our data suggest that the inflammation with cytokine expression is induced after alkali attachment to the cornea and that at least some portion of cytokines is secreted from the corneal tissue; however, infiltrations of inflammatory cells into the cornea may be needed for an explosive increase of the cytokines. Similar to the corneal epithelial wound healing observed in rats after wound generation by surgical ablation, PPARδ was not observed in the corneal epithelial cells before and immediately after alkali attachment (Figure 7, H–K) and was up-regulated in the corneal epithelial cells of the corneas that received alkali attachment at the points of 8 hours and 1 and 7 days after the keratitis was induced (Figure 7, L–O, R, and S). Furthermore, the up-regulation of PPARδ disappeared at the points of 3 days showing its recurrent up-regulation (Figure 7, P–Q) and returned its initial level at 21 days (Figure 7, T–U). Thus, the period of up-regulation observed in the induced keratitis model was much longer than the period observed in the corneas that received surgical ablation (Figure 1, B–L), suggesting that sustained inflammation might cause a longer period of PPARδ up-regulation.

During the period of keratitis-associated inflammation, TUNEL-positive cells were detected in the corneal epithelia at 8 hours and at 1, 3, and 7 days after the alkali attachment (Figure 8, C–F), suggesting that the apoptotic cell death might be induced by the inflammation of the ocular surfaces in alkali-induced keratitis. On the other hand, TUNEL staining showed that the number of positive cells peaked at 8 hours after alkali attachment, whereas the peak of cytokine secretion was at 1 day. We theorize that this discrepancy (ie, the peak of TUNEL staining was after 8 hours when the cytokine levels only peaked after 1 day) may be
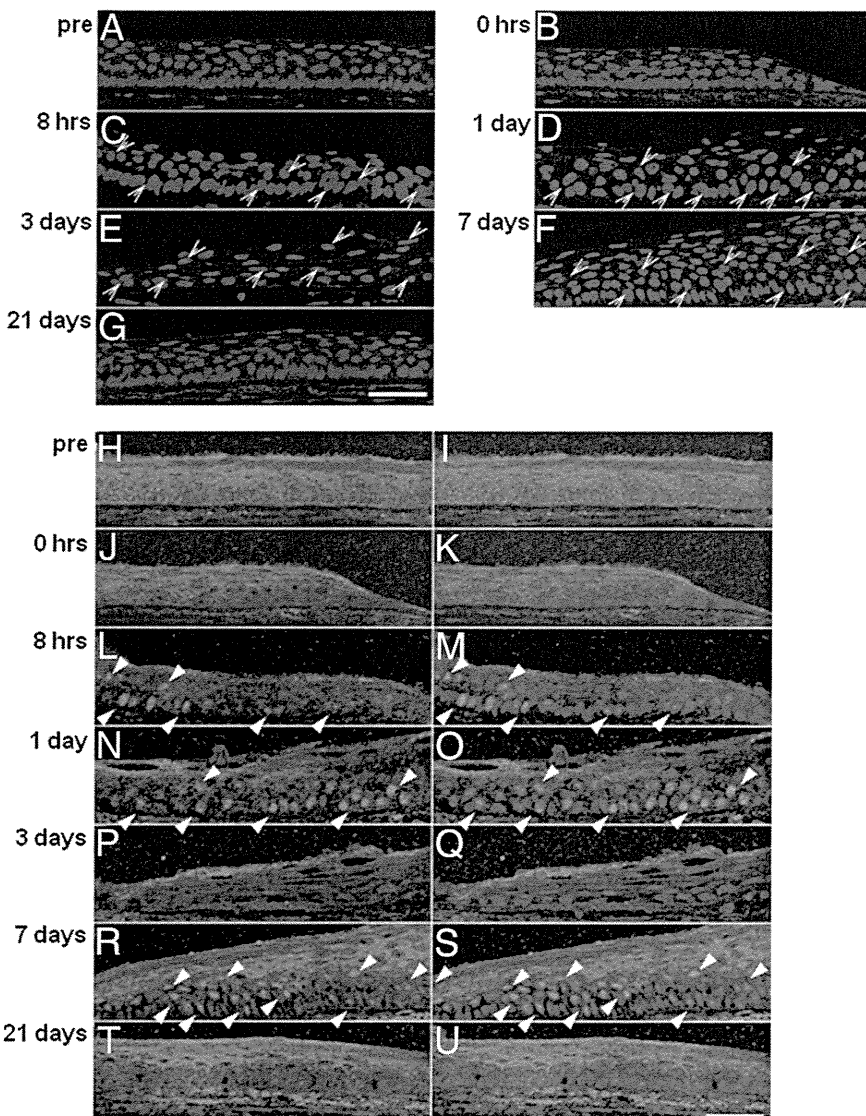
Figure 7. Analyses of the wound-healing process in rat corneas with alkali-induced keratitis (continued from Figure 6). Representative photographs of immunofluorescent staining for IL-1β showing before (**A**) or 0 hours (**B**), 8 hours (**C**), 1 day (**D**), 3 days (**E**), 7 days (**F**), or 21 days (**G**) after receiving alkali attachment in the rat corneal epithelia during wound healing. The blue and red staining represents the cellular nuclei and IL-1β, respectively, and typical staining of IL-1β is indicated by **open arrowheads**. IL-1β was expressed in cell nuclei at 8 hours and 1, 3, and 7 days after alkali attachment. Representative photographs of immunofluorescent staining for PPARδ showing before (**H** and **I**) or 0 hours (**J** and **K**), 8 hours (**L** and **M**), 1 day (**N** and **O**), 3 days (**P** and **Q**), 7 days (**R** and **S**), or 21 days (**T** and **U**) after the treatment, respectively, in the rat corneal epithelia during wound healing. The blue and green staining represents the cellular nuclei and PPARδ, respectively. Photographs **H, J, L, N, P, R**, and **T** and photographs **I, K, M, O, Q, S**, and **U** show immunofluorescent microscopy for PPARδ and those merged with DAPI staining, respectively. Typical staining of PPARδ is indicated by **closed arrowheads**, and PPARδ was obviously expressed in cell nuclei at 8 hours and 1 and 7 days after alkali attachment. Scale bar = 50 μm.

caused by apoptosis inducers, including other pro-inflammatory cytokines being secreted at 8 hours into the cornea, although they had not reached their peaks; then, they continuously induced apoptosis of the corneal epithelial cells from 8 hours until 21 days.

Temporal Expression of PPARδ in an ex Vivo Human Corneal Epithelial Wound Model

To elucidate the involvement of PPARδ in human corneal epithelial wound healing, we evaluated the expression of PPARδ in a human corneal epithelial wound model ex vivo. First, we demonstrated the expression of PPAR isoforms in human corneal epithelia obtained from healthy quiescent human corneal tissues immediately postmortem, and cDNA samples were separately prepared from their peripheral and central regions. PPAR α, δ, and γ mRNAs were detected in the peripheral region of the corneal epithelia, whereas only expressions of PPAR α and δ mRNAs were observed in the central region of them (Figure 9A). The

corneal epithelial wounds generated by surgical ablation on the enucleated human corneoscleral tissues healed slowly, and re-epithelialization of those samples was incomplete, thus showing insufficient recovery of the cell layer after 48 hours of culture (Figure 9, F and G), which is in contrast to the in vivo experiment using an animal model (Figure 1). During such partial re-epithelialization processes ex vivo, the staining of PPARδ was not detected in the intact corneal epithelia before surgical ablation or in the corneal epithelia immediately and at 24 hours of culture after the generation of the wounds. However, some PPARδ signals were observed on the nucleus of corneal epithelia cells cultured for 48 hours after the ablations (Figure 9, F and G).

Next, human corneoscleral tissues were used to investigate the effect of inflammation on PPARδ protein expression. After a 24-hour culture of the tissues in the presence of 10 ng/mL TNF-α, obvious PPARδ signals were detected in the corneal epithelia of those samples (Figure 9H). A 24-hour culture of the tissues in the absence of TNF-α also caused the expression of PPARδ in their cor-
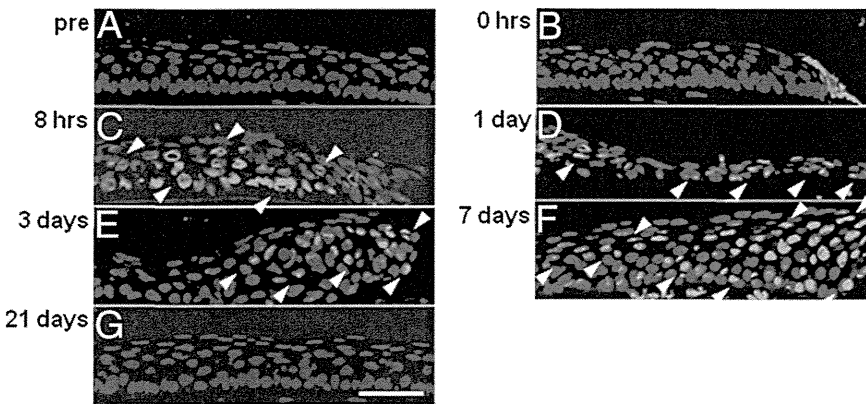
Figure 8. Analyses of the wound-healing process in rat corneas with alkali-induced keratitis (continued from Figure 7). Representative photographs of TUNEL staining showing before (A) or 0 hours (B), 8 hours (C), 1 day (D), 3 days (E), 7 days (F), or 21 days (G) after receiving alkali attachment in the rat corneal epithelia during wound healing. The blue and green staining represents cellular nuclei and TUNEL-positive staining, respectively. Typical TUNEL-positive staining is indicated by **white arrowheads** and was observed on the cell nuclei at 8 hours and 1, 3, and 7 days after alkali attachment. Scale bar = 50 μm.

neal epithelia (Figure 9I), which was unexpected. However, the frequencies of staining seemed to be up-regulated in the cytokine-treated tissues compared with the nontreated tissues (Figure 9H). To confirm the up-regulation of PPARδ, we tried to evaluate the effect of cytokines on the expression of PPARδ using cultured HCECs

in vitro. As a result, the marked up-regulation of PPARδ could be detected in the cells treated with the cytokines (Figure 9, J and K). On the other hand, TUNEL staining showed that the treatment with TNF-α clearly caused DNA fragmentations, thus suggesting that the cytokine induced the cell apoptosis (Figure 9M).
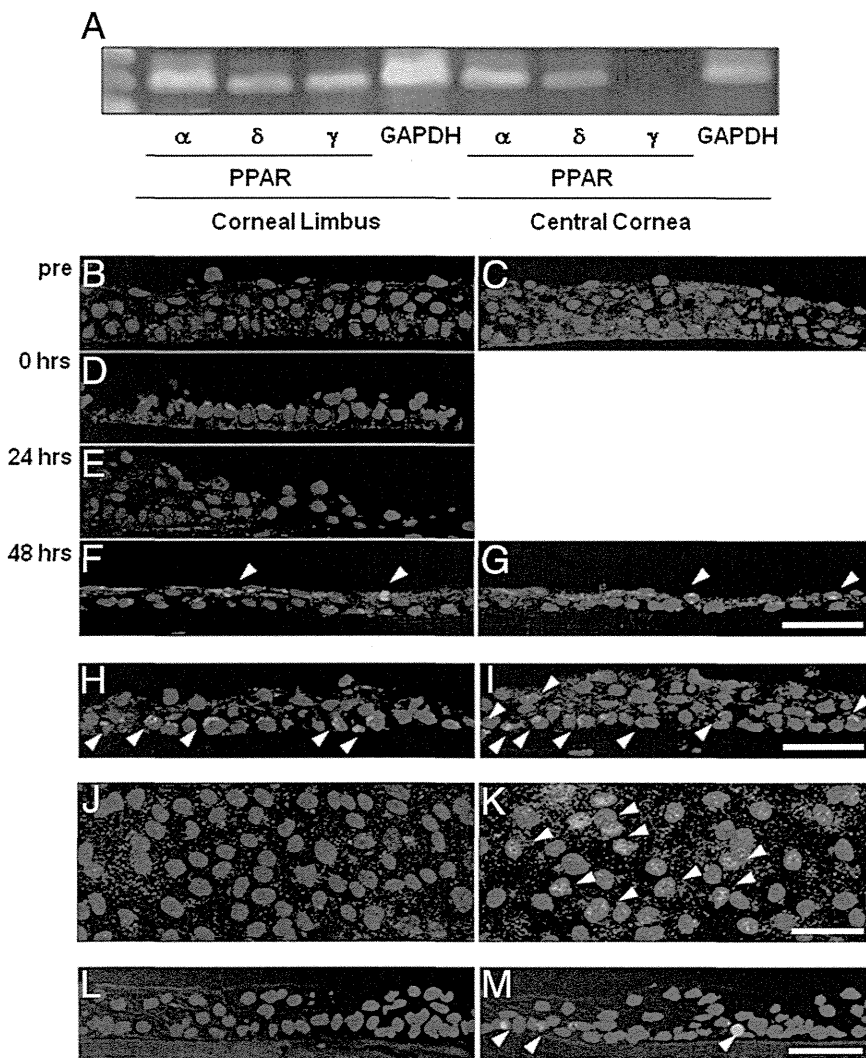

Figure 9. A: RT-PCR for PPARs in human corneal epithelial tissue using total RNAs separately prepared from the limbus and central region of the corneas. GAPDH indicates glyceraldehyde-3-phosphate dehydrogenase. **B–G:** Representative photographs of immunofluorescent staining for PPARδ in corneal epithelia on enucleated human corneoscleral samples during re-epithelialization *ex vivo* after mechanical abrasion. The blue and green staining represents the cell nuclei and PPARδ, respectively. Typical staining of PPARδ is indicated by **white arrowheads. B:** Corneal periphery before wound generation. **C:** Edge of the epithelial wound before wound generation. **D:** Edge of the epithelial wound immediately after wound generation. **E:** Edge of the epithelial wound at 24 hours after wound generation. **F:** Area next to the epithelial wound edge at 48 hours after wound generation. **G:** Edge of the epithelial wound at 48 hours after wound generation. In the abraded tissues incubated for 24 hours, the number of corneal epithelial cells was increased at the edge of the wounds, whereas PPARδ staining was not observed. On the other hand, limited, yet obvious, PPARδ staining was observed on the cell nuclei located at the peripheral region and the area next to the wound edge in the abraded tissues incubated for 48 hours. Scale bar = 50 μm. **H** and **I:** Representative photographs of immunofluorescent staining for PPARδ in corneal epithelia on enucleated human corneoscleral pieces during treatment without (**H**) or with (**I**) 10 ng/mL TNF-α *ex vivo.* The blue and green staining represents the cell nuclei and PPARδ, respectively. Typical staining of PPARδ is indicated by **white arrowheads.** Scale bar = 50 μm. **J** and **K:** Representative photographs of immunofluorescent staining for PPARδ in primary cultured HCECs during treatment without (**J**) or with (**K**) 20 ng/mL TNF-α *in vitro.* The blue and green staining represents the cell nuclei and PPARδ, respectively. Typical staining of PPARδ is indicated by **white arrowheads.** Scale bar = 50 μm. **L** and **M:** Representative photographs of TUNEL staining in corneal epithelia on enucleated human corneoscleral samples during treatment without (**L**) or with (**M**) 10 ng/mL TNF-α *ex vivo.* The blue and green staining represents the cell nuclei and TUNEL-positive staining, respectively. Typical TUNEL-positive staining is indicated by **white arrowheads** (**M**). Scale bar = 50 μm.
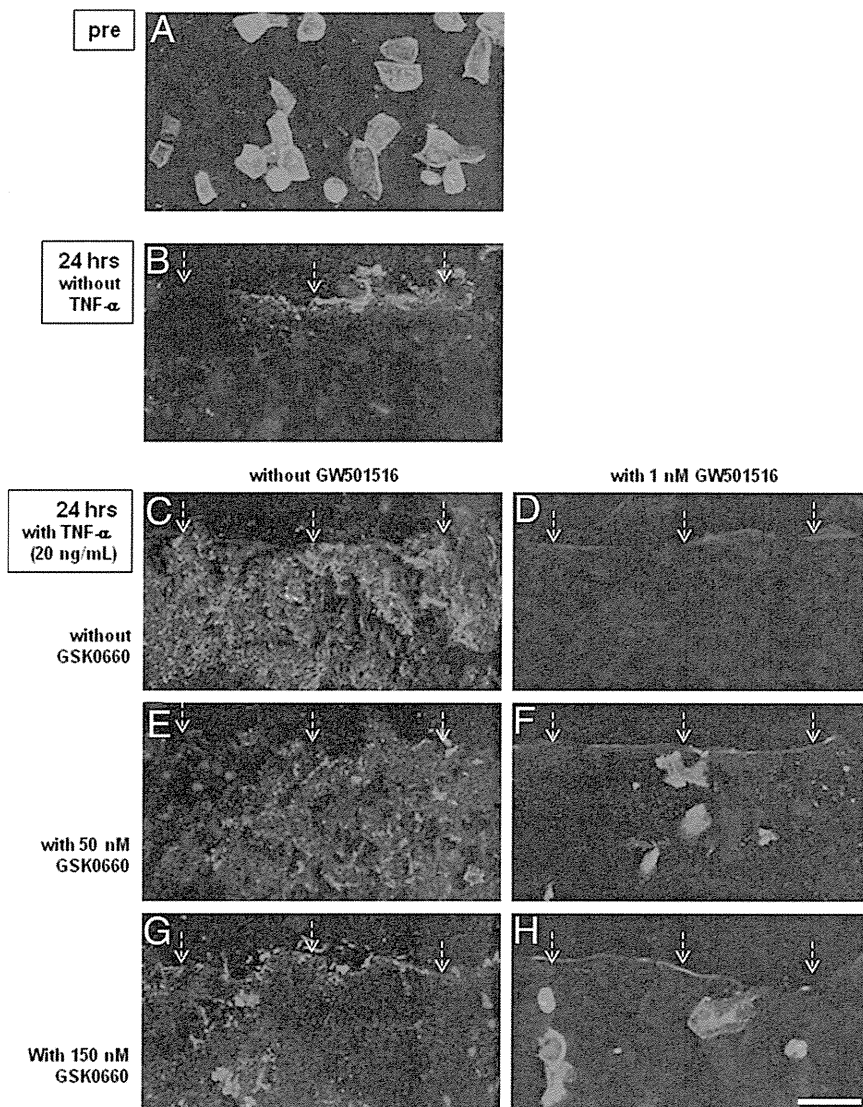
Figure 10. Representative photographs of immunofluorescent staining for annexin V in corneal epithelia on enucleated human corneoscleral samples during re-epithelialization *ex vivo* after mechanical abrasion. The green and red staining represents annexin V and the propidium iodide staining of cellular nuclei, respectively, and shows the cell death. The edges of corneal epithelial wounds are indicated by fine-dotted **white arrows (B–H)**; the top side of each photograph is the center of the cornea, and the bottom side is the corneal limbus. The photographs show the corneal epithelia before wound generation (**A**), at 24 hours after wound generation with no additional treatments (**B**), at 24 hours after wound generation with stimulation by 20 ng/mL TNF-α (**C**), at 24 hours after wound generation with stimulation by 20 ng/mL TNF-α and pretreatment of 1 nmol/L GW501516 (**D**), at 24 hours after wound generation with stimulation by 20 ng/mL TNF-α and pretreatment of 50 nmol/L GSK0660 (**E**), at 24 hours after wound generation with stimulation by 20 ng/mL TNF-α and pretreatments of 50 nmol/L GSK0660 plus 1 nmol/L GW501516 (**F**), at 24 hours after wound generation with stimulation by 20 ng/mL TNF-α and pretreatment of 150 nmol/L GSK0660 (**G**), and at 24 hours after wound generation with stimulation by 20 ng/mL TNF-α and pretreatments of 150 nmol/L GSK0660 plus 1 nmol/L GW501516 (**H**). Scale bar = 50 μm.

Effect of a PPARδ Agonist on TNF-α–Induced HCEC Death in an ex Vivo Model

Because the inflammatory stimulation caused the upregulation of PPARδ and DNA fragmentation of corneal epithelial cells, and because the PPARδ agonist, GW501516, could inhibit inflammatory cytokine-induced DNA fragmentation, we next evaluated the effect of GW501516 on TNF-α–induced corneal epithelial cell death using an *ex vivo* human corneoscleral tissue culture system (Figure 10). In this system, the cell death was detected as annexin V staining of their membranes and as propidium iodide staining of their nuclei. The corneal epithelial cell death was observed in noncultured corneoscleral tissues (Figure 10A), suggesting that the storage of the tissues for 4 to 5 days at 4°C caused them to die. After the 24-hour culture of the tissues, which had received surgical ablation of the corneal epithelia, cell death was observed only faintly at the edge of the corneal epithelial wound as annexin V staining (Figure 10B), thus showing a lower amount of cell death. However, when the tissues were

treated with TNF-α, marked corneal epithelial cell death, which was observed as both annexin V– and propidium iodide–positive cells, was observed (Figure 10C). According to the results *in vitro* (Figure 5A), the TNF-α–induced corneal epithelial cell death was clearly inhibited by the pretreatment of those cells with the concentration of GW501516 (Figure 10D). The use of GSK0660, a specific PPARδ antagonist, did not exhibit anti-cell death effects (Figure 10, E and G). Interestingly, the effect of GW501516 on the TNF-α–induced cell death was partially inhibited by cotreatments of the concentrations of GSK0660 (Figure 10, F and H), thus showing, at least partially, the effect of GW501516 on cell death via PPARδ.

Particular Expression Pattern of PPARδ in Diseased Human Corneas

To investigate the particular expression pattern of PPARδ, diseased corneas, in which the corneal epithelial wounds were clearly observed by fluorescein testing (Figure 11,